How spin-flip scattering influences the minigap in a S-N junction

Rapport de travail pratique pour l'obtention du
Diplôme de Physicien EPFL

Octobre 2004 – Février 2005

Benoît Crouzy

Responsable EPFL:	Pr Dmitri Ivanov
Responsables ETHZ:	Dr Elena Bascones
	Pr Manfred Sigrist

Acknowledgements

At the end of this diploma, I would like to thank the people who have allowed me to work on this subject. I am particularly grateful for the support and time Elena Bascones and Dmitri Ivanov offered me. I also thank Manfred Sigrist for giving me the opportunity to accomplish this diploma at the ETH Zurich.

Contents

1 Introduction **6**

2 General context: description of the S-N junction **6**
2.1 Bogoliubov-de Gennes equations 6
2.2 Diffusive regime 8
2.3 Model of the S-N junction 8
2.4 Andreev reflection 9

3 Green functions in the BCS theory **10**
3.1 Gor'kov equations 10
3.2 Real time formulation 11
3.3 Scattering on impurities: self-energy 12
3.4 Quasiclassical theory 14
3.4.1 Eilenberger equations 14
3.4.2 Usadel equations 15
3.5 Spin-flip scattering 17
3.6 Pair breaking effect of a magnetic field 19

4 Solution for a homogeneous superconductor **21**

5 Usadel equations for the S-N system **23**
5.1 Boundary conditions for the S-N system 23
5.2 Minigap in the DoS of the N-part 24

6 Linearization of the Usadel equations **25**
6.1 Linearization close to $\theta = \frac{\pi}{2}$ 25
6.2 Linearization close to $\theta = 0$ 27

7 First integral **28**
7.1 Gap solution 28
7.2 Zero-energy gapless solution 31
7.3 Dependance of the minigap on Γ_{sf} 33
7.3.1 Small Γ_{sf} limit 33
7.3.2 Gap curve close to Γ_{sf}^c 33
7.3.3 Numerical gap curve 34

8 Zero-energy solution for finite Γ_{sf} **35**

9 Summary **39**

A Exact zero-energy solution for finite Γ_{sf} **42**

B Exact solution for $\Gamma_{sf} = 0$ **45**

C Gap curve close to Γ_{sf}^c **46**

1 Introduction

Hybrid structures, made of superconducting and non-superconducting elements in contact with each other, have been studied since the microscopic BCS theory of superconductivity (1957) exists. Recent technical progress has made possible the production of small samples ($\sim 1\mu$m) and coherence at mesoscopic scale is theoretically better understood. Practical applications of such structures [16] are for example SQUID Josephson magnetometers, which allow very sensitive magnetic field measurement or S-N devices used in photodetection.

A superconductor in contact with a normal metal modifies the behaviour of the electrons in the normal part ("proximity effect"). The electrons in the adjacent normal metal will exhibit superconducting properties like:

- apparition of an energy gap in the density of states
- modification of the conductance (strongly dependent on energy)
- screening of a magnetic field

The scale at which these properties can be observed is a so called "mesoscopic scale", characterised by the presence of a sufficient number of particles to use statistical methods but still showing a non negligible phase coherence effect. In this work, we will study the influence of inelastic and spin-flip scattering on the electron density of states in diffusive S-N junctions.

2 General context: description of the S-N junction

2.1 Bogoliubov-de Gennes equations

The effect of superconductivity is related to the presence of an interaction between the electrons of the material, generally mediated by an exchange of phonons (the electrons interact with the vibrations of the lattice). This interaction makes the electronic system unstable and the electrons condense in Cooper pairs. Therefore, to describe superconducting materials, we consider a Hamiltonian containing an attractive interaction term H_I in addition to the usual kinetic part H_0 [2]. Here, we neglect the role of the Coulomb interaction and treat the electrons as a Fermi liquid:

$$H = H_0 + H_I \tag{2.1}$$

If the interaction is weak compared to the Fermi energy of the electrons, it is reasonable to consider a point like pairing interaction $U(\mathbf{r}_1 - \mathbf{r}_2) =$

$\frac{g}{2}\delta(\mathbf{r}_1 - \mathbf{r}_2)$. The second quantised expression for the BCS Hamiltonian is:

$$H = \int \sum_{\alpha} \psi_{\alpha}^{\dagger} \frac{-\nabla^2}{2m} \psi_{\alpha} + \sum_{\alpha\beta} \frac{g}{2} \psi_{\beta}^{\dagger} \psi_{\alpha}^{\dagger} \psi_{\alpha} \psi_{\beta} + \sum_{\alpha,\beta} \psi_{\alpha}^{\dagger} u_{\alpha\beta}(\mathbf{r}) \psi_{\beta} \, d^3r \tag{2.2}$$

where $\Psi_{\sigma}^{\dagger}(\mathbf{r})$ are the usual field operators (creation of an electron with spin σ at the position $\mathbf{r}$). The external potential $u(\mathbf{r})$ includes impurities in the model and will be discussed in more details later.
The interaction part of the Hamiltonian can be simplified and reduced to a quadaratic form in the field operators [21]. The idea is to replace the interaction by an average single-particle potential (mean field approximation):

$$H_M = \int \left[\Delta(\mathbf{r}) \psi_{\uparrow}^{\dagger} \psi_{\downarrow}^{\dagger} + \Delta^{\star}(\mathbf{r}) \psi_{\downarrow} \psi_{\uparrow} \right] d^3r \tag{2.3}$$

$$\Delta(\mathbf{r}) = |g(\mathbf{r})| \langle \psi_{\downarrow} \psi_{\uparrow} \rangle \tag{2.4}$$

The spatial dependence of $g(\mathbf{r})$ allows us to describe systems such as S-N junctions: in the normal part, the interaction responsible for the formation of Cooper pairs vanishes.
At this point, we have a quadratic Hamiltonian in the fields operators which is non-diagonal. To diagonalize this Hamiltonian, we introduce the canonical (Bogoliubov) transformation:

$$\psi_{\uparrow}(\mathbf{r}) = \sum_{n} \gamma_{n\uparrow} u_n(\mathbf{r}) - \gamma_{n\downarrow}^{\dagger} v_n^{\star}(\mathbf{r}) \tag{2.5}$$

$$\psi_{\downarrow}(\mathbf{r}) = \sum_{n} \gamma_{n\downarrow} u_n(\mathbf{r}) + \gamma_{n\uparrow}^{\dagger} v_n^{\star}(\mathbf{r}) \tag{2.6}$$

From the equations of motion for the initial field operators Ψ, we obtain the equations for the coefficients of the transformation u_n and v_n which are chosen to make the Hamiltonian diagonal. These coefficients are the eigenfunctions, with corresponding eigenvalues E_n, of the system (Bogoliubov-de Gennes equations):

$$i\hbar\partial_t \begin{pmatrix} u \\ v \end{pmatrix} = \begin{pmatrix} H_0 - \mu & \Delta \\ \Delta^{\star} & -H_0 + \mu \end{pmatrix} \begin{pmatrix} u \\ v \end{pmatrix} \tag{2.7}$$

which corresponds to a Schrödinger equation for the two component wave function (u, v). It is possible to solve these equations only for simple (ballistic) systems. In section (3) we will review the Green function formalism of the BCS theory which is of course equivalent to the Bogoliubov-de Gennes equations but allows to include more complicated systems like dirty superconductors in the formalism.

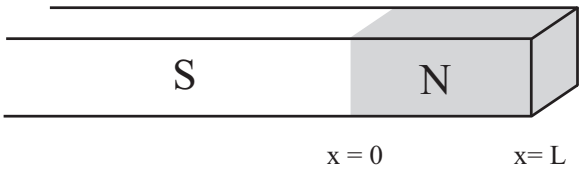

Figure 1: Semi-infinite S-N junction

2.2 Diffusive regime

In this work, we will study diffusive S-N junctions. In the diffusive regime, the motion of electrons is governed by scattering on impurity atoms. We define l_e, the mean free path between two elastic scatterings. The spatial extension associated with a time interval t is given by:

$$L = \sqrt{Dt} \tag{2.8}$$

where the diffusion constant D is given (for a three dimensional geometry) by:

$$D = \frac{1}{3} v_f l_e \tag{2.9}$$

Relation (2.8) has to be distinguished from the ballistic case where:

$$L = v_f t \tag{2.10}$$

It is also possible to define the characterstic length L_ϵ associated with an energy ϵ by:

$$L_\epsilon = \sqrt{\frac{\hbar D}{\epsilon}} \tag{2.11}$$

2.3 Model of the S-N junction

We consider a narrow S-N junction. The system consists on a semi-infinite superconductor ($x = -\infty$ to 0) connected to a finite length normal part ($x = 0$ to L) by a transparent interface (no potential barrier). Without further specifications, we will consider that there is no external magnetic field and set the phase of the order parameter to zero (only one superconducting terminal). Finally we consider a step-like pair interaction $\Delta(x) = \Delta\Theta(-x)$ at the interface.

We assume that the width of the system is constant and of the order of the elastic mean free path l_e. In this narrow geometry (in the literature: "quasi 1D junction"), there is no diffusive motion of the electrons in the transverse directions. The idea is that in the diffusive limit, the elastic mean free path satisfies the conditions

$$l_e \ll \xi \tag{2.12}$$

and

$$l_e \ll L \tag{2.13}$$

where ξ is the coherence length of the superconducting material. If these conditions are satisfied, l_e is smaller than the relevant length scales of our system and therefore we can neglect the variations of the physical quantities along transverse directions for a junction of a width $\sim l_e$.

2.4 Andreev reflection

The microscopic mechanism resulting in the presence of a finite Cooper pair amplitude in the normal part of the junction is a particular type of scattering at the S-N interface. At low energy, the electrons in the N-part with an excitation energy ϵ below the superconducting gap Δ cannot cross the interface (no single particle state available in the superconductor below the gap). In our model of the junction, we consider that there is no potential barrier, therefore incident electrons cannot be directly reflected either (momentum conservation). Therefore, an incident electron will be retro-reflected as a hole with energy $-\epsilon$, opposite spin and a Cooper pair is transmitted through the interface. The reflection of a hole is equivalent to the absorption of a second electron by the interface. This results in the diffusion of electron pairs ("Andreev pairs") in the normal metal. These pairs are not due to the presence of an hypothetical interaction in the normal metal but to the scattering of Andreev pairs from the S-N interface.
This pair scattering is perfect only at the Fermi level. The reflected hole corresponding to an electron with wave vector $\mathbf{k}_e = \mathbf{k}_F + \mathbf{q}$, has a wave vector $\mathbf{k}_h = \mathbf{k}_F - \mathbf{q}$. This wave vector mismatch $2\mathbf{q}$ will result in an imperfect Andreev pairing, the mismatch of the trajectories growing with the distance to the interface and destroying the correlation. For an electron with energy $E_F + \epsilon$, the coherence length of the Andreev pairs L_ϵ is given by relation (2.11). If we consider a sample of length L, this relation gives us the corresponding characteristic correlation energy (Thouless energy)

$$E_{Th} = \frac{\hbar D}{L^2}. \tag{2.14}$$

This simple description is valid as long as pair breaking effect (scattering on magnetic impurities) or inelastic scattering can be neglected. These type of scattering become important if the spin-flip or the inelastic mean free path (respectively L_φ and L_{in}) are smaller than the length of the N-part of the sample L.

3 Green functions in the BCS theory

3.1 Gor'kov equations

The formulation of the BCS theory in terms of Green functions derived by [3] furnishes efficient tools: relevant physical quantities can be directely obtained once the electron Green function has been calculated. To describe finite temperature systems, one introduces imaginary-time Matsubara Green functions :

$$G_{\alpha\beta}(\mathbf{r}_1,\tau_1;\mathbf{r}_2,\tau_2) = Tr\left[exp\left(\frac{\Omega+\mu\hat{N}-\hat{H}}{T}\right)T_\tau\Psi_\alpha(r_1,\tau_1)\Psi^\dagger_\beta(r_2,\tau_2)\right], \tag{3.1}$$

where $t=-i\tau$, μ is the chemical potential, Ω the thermodynamic potential and $\hat{H}$ the BCS Hamiltonian (2.2) (we neglect the role of the Coulomb interaction between electrons). Later we will also use the notation $\mathrm{x}=(\mathbf{r},\tau)$.

The fact that we work with an imaginary time allows to order the exponential factor with the time ordering symbol T_τ when $-\frac{1}{T}<\tau_1-\tau_2<\frac{1}{T}$. Therefore, it is possible to use the Wick theorem to separate products of field operators.
Using the microscopic BCS Hamiltonian (2.2) to compute time derivatives of the Green function and the Wick theorem to separate the interaction term, one gets the Gor'kov equations for the matrix Green function (Nambu space):

$$\check{\mathcal{G}}^{-1}(\mathrm{x}_1)\check{G}(\mathrm{x}_1,\mathrm{x}_2) = \check{1}\delta(\mathrm{x}_1,\mathrm{x}_2) \tag{3.2}$$

$$\check{G}(\mathrm{x}_1,\mathrm{x}_2)\overline{\check{\mathcal{G}}}^{-1}(\mathrm{x}_2) = \check{1}\delta(\mathrm{x}_1,\mathrm{x}_2) \tag{3.3}$$

where

$$\check{G}(\mathrm{x}_1,\mathrm{x}_2) = \begin{pmatrix} G(\mathrm{x}_1,\mathrm{x}_2) & F(\mathrm{x}_1,\mathrm{x}_2) \\ -F(\mathrm{x}_1,\mathrm{x}_2)^\dagger & \bar{G}(\mathrm{x}_1,\mathrm{x}_2)\end{pmatrix} \tag{3.4}$$

and

$$\check{\mathcal{G}}^{-1} = \check{\tau}_3\frac{\partial}{\partial\tau}+\check{H} \tag{3.5}$$

$$\overline{\check{\mathcal{G}}}^{-1} = -\check{\tau}_3\frac{\partial}{\partial\tau}+\check{H} \tag{3.6}$$

$$\check{H} = \begin{pmatrix} -\frac{\nabla^2}{2m}-\mu & -\Delta \\ \Delta^\star & -\frac{\nabla^2}{2m}-\mu\end{pmatrix} \tag{3.7}$$

The "check" is used to denote matrices in the Nambu space, and $\check{\tau}_i$ are the Pauli matrices in this space. This theory is symmetrical in terms of particle-hole, the function $\bar{G}$ describing the propagation of a hole:

$$\bar{G}(\mathrm{x}_1,\mathrm{x}_2) = -\langle T_\tau\Psi(\mathrm{x}_1)^\dagger\Psi(\mathrm{x}_2)\rangle_{stat} = G(\mathrm{x}_2,\mathrm{x}_1) \tag{3.8}$$

with $\langle \ldots \rangle_{stat}$ given by (3.1).
The anomalous parts of the Green function

$$F(\mathrm{x}_1, \mathrm{x}_2) := \langle T_\tau \Psi(\mathrm{x}_1)\Psi(\mathrm{x}_2)\rangle_{stat} \tag{3.9}$$
$$F^\dagger(\mathrm{x}_1, \mathrm{x}_2) := \langle T_\tau \Psi^\dagger(\mathrm{x}_1)\Psi^\dagger(\mathrm{x}_2)\rangle_{stat} \tag{3.10}$$

are related to the order parameter Δ by the coupling constant g which appears in the interaction term of the BCS Hamiltonian $U(\mathbf{r}_1 - \mathbf{r}_2) = \frac{g}{2}\delta(\mathbf{r}_1 - \mathbf{r}_2)$ following relation (2.4).

In equations (3.2) and (3.3) the spin indices no longer appear. But it is important to notice that the Green functions G and F have a different spin structure. Since the interaction between electrons is spin independent we can write:

$$G_{\alpha\beta}(\mathrm{x}_1, \mathrm{x}_2) = \delta_{\alpha\beta}\, G(\mathrm{x}_1, \mathrm{x}_2) \tag{3.11}$$

and for an s-wave pairing (even parity in the orbital space), the Cooper pairing can only occur between electrons with opposite spin. Therefore we write:

$$F_{\alpha\beta}(\mathrm{x}_1, \mathrm{x}_2) = i\sigma^{(2)}_{\alpha\beta}\, F(\mathrm{x}_1, \mathrm{x}_2). \tag{3.12}$$

We use the notation $\sigma^{(i)}$ for the Pauli matrix in the spin-space to avoid confusion with the Pauli matrix in the Nambu space $\tau^{(i)}$.
In the following, we will often express the Green function in terms of its Fourier components (frequency representation) and in the momentum space.

$$\check{G}_{\omega_n}(\mathbf{r}_1, \mathbf{r}_2) = \int_0^{\frac{1}{T}} e^{i\omega_n \tau} \check{G}(\mathbf{r}_1, \mathbf{r}_2, \tau), \tag{3.13}$$

where $\omega_n = (2n+1)\pi T$ are the Matsubara frequencies and $\tau = \tau_1 - \tau_2$. For the momentum representation of the Green function, we write:

$$\check{G}(\mathbf{r}_1, \mathbf{r}_2) = \int \frac{d^3p}{(2\pi)^3} \int \frac{d^3p'}{(2\pi)^3} \check{G}(\mathbf{p}, \mathbf{p}') e^{i\mathbf{p}\mathbf{r}_1 - i\mathbf{p}'\mathbf{r}_2}. \tag{3.14}$$

3.2 Real time formulation

Until now, we have been working with imaginary time to derive the Green function formalism. Now, we define the advanced and retarded real time Green functions:

$$\begin{aligned} G^R(\mathrm{x}_1, \mathrm{x}_2) &= i\langle T_\tau \Psi(\mathrm{x}_1)\Psi^\dagger(\mathrm{x}_2) + \Psi^\dagger(\mathrm{x}_1)\Psi(\mathrm{x}_2)\rangle_{stat} && \tau_1 > \tau_2 \\ G^R(\mathrm{x}_1, \mathrm{x}_2) &= 0 && \tau_1 < \tau_2 \end{aligned}$$

and

$$\begin{aligned} G^A(\mathrm{x}_1, \mathrm{x}_2) &= -i\langle T_\tau \Psi(\mathrm{x}_1)\Psi^\dagger(\mathrm{x}_2) + \Psi^\dagger(\mathrm{x}_1)\Psi(\mathrm{x}_2)\rangle_{stat} && \tau_1 < \tau_2 \\ G^A(\mathrm{x}_1, \mathrm{x}_2) &= 0 && \tau_1 > \tau_2 \end{aligned}$$

Using these definitions and working in the frequency representation (3.13), one can show that the real frequency Green functions $G_\epsilon^{R(A)}$ are the analytical continuation of the Matsubara Green function G_{ω_n} from the positive, respectively negative, imaginary axis:

$$G_{\omega_n} = G^R_{i\omega_n},\ \omega_n > 0 \tag{3.15}$$

$$G_{\omega_n} = G^A_{i\omega_n},\ \omega_n < 0 \tag{3.16}$$

At this point, it is important to mention the connection between the Green function formalism and the Bogoliubov-de Gennes equations. The real time Green functions can be expressed in terms of the particle u and hole v wave functions solution of the BdG equation (2.7):

$$G^{R(A)}_{i\omega_n} = \sum_N \frac{\begin{pmatrix} u \\ v \end{pmatrix} \begin{pmatrix} u^\star & v^\star \end{pmatrix}}{E_N - i\omega_n \mp i\delta} \tag{3.17}$$

where the energies E_N are the eigenvalues of the BdG equations (2.7).

3.3 Scattering on impurities: self-energy

In this section, we briefly review how electron scattering on random impurity atoms is introduced in the Green function formalism of the BCS theory (see for e.g. [1] and [22] for a detailed description). Consider an impurity at the position $\mathbf{r_a}$. We write the corresponding interaction potential $u(\mathbf{r} - \mathbf{r_a})\check{1}$ ($\check{1}$ denotes the unity matrix in the Nambu space) and assume that:

- The scattering potential u is small compared to the Fermi energy E_F (Born approximation).
- It is possible to average over positions of the impurities (random impurities).
- Scattering is elastic.

Within this framework, it is possible to treat the interaction as a perturbation and to express the Green function of the interacting electrons as a Dyson serie from the Green function $\check{G}^{(0)}$ of the unperturbed system. Incorporating the diagrams with scattering on differents atoms into the chemical potential μ and neglecting the contribution of diagrams with more than two scattering per atom (Born approximation), we only keep the diagrams with two scattering per atom. It can be shown [1] that the contribution of the diagrams where the lines connecting scattering on the same atom intersect is reduced by a factor $\frac{1}{p_F l_e}$, which is small for metals. After summation of

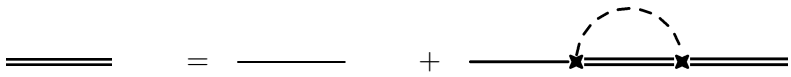

Figure 2: Graphical Dyson equation

all the relevant diagrams, one gets a Dyson equation for the matrix Green function:

$$\check{G}(\mathbf{p},\mathbf{p}') = \check{G}^{(0)}(\mathbf{p},\mathbf{p}') + \int \check{G}^{(0)}(\mathbf{p},\mathbf{p}_1)\check{\Sigma}(\mathbf{p}_1,\mathbf{p}_2)\check{G}(\mathbf{p}_2,\mathbf{p}')d^3p_1 d^3p_2, \quad (3.18)$$

where we introduced the self energy matrix $\check{\Sigma}$ given in the Fourier representation by:

$$\check{\Sigma}(\mathbf{p},\mathbf{p}') = n_{imp}\int \frac{dp_1^3}{(2\pi)^3}\,\sigma(\mathbf{p},\mathbf{p}_1)\,\check{G}(\mathbf{p}_1,\mathbf{p}_1-\mathbf{p}+\mathbf{p}'). \quad (3.19)$$

The scattering cross section $\sigma(\mathbf{p},\mathbf{p}')$ is related to the impurity potential u by the relation (Born approximation):

$$\left|u(\mathbf{p}-\mathbf{p}')\right|^2 = \frac{2v_F}{\nu_0}\sigma(\mathbf{p},\mathbf{p}'), \quad (3.20)$$

with $\nu_0 = mp_F/2\pi^2$ the density of states per one spin projection in the normal state. Finally, we introduce the scattering mean free time τ_e:

$$\sigma_{tot} n_{imp} \underbrace{v_F\tau_e}_{l_e} = 1. \quad (3.21)$$

The Dyson equation (3.18) is equivalent to the Gor'kov equation in the momentum representation:

$$[(\check{\mathcal{G}}^{-1}_{clean} - \Sigma) * \check{G}]_{\mathbf{p},\mathbf{p}'} = (2\pi)^3\delta(\mathbf{p}-\mathbf{p}')\check{1}. \quad (3.22)$$

with

$$[\check{A} * \check{B}]_{\mathbf{p},\mathbf{p}'} = \int \frac{d^3p_1}{(2\pi)^3}\check{A}(\mathbf{p},\mathbf{p}_1)\check{B}(\mathbf{p}_1,\mathbf{p}'). \quad (3.23)$$

3.4 Quasiclassical theory

If we consider conventional (low temperature) superconductors, the order parameter Δ is much smaller than the Fermi energy ($\frac{\Delta}{E_F} \sim 10^{-3}$). In this case, the quasiclassical approximation simplifies the calculation of the Green function (which is often a difficult task working with the Gor'kov formalism). The idea is that the scale of variation for superconducting properties (coherence length ξ) is much larger than the Fermi wavelength:

$$\frac{1}{p_F \xi} \sim \frac{\Delta}{E_F} \ll 1 \tag{3.24}$$

The superconducting properties are related to the contributions of the Green functions with momenta close to the Fermi surface ($\Delta \ll E_F$). Therefore, we introduce the notation :

$$\check{G}(\mathbf{p}_1, \mathbf{p}_2) = \check{G}(\mathbf{p} + \frac{\mathbf{k}}{2}, \mathbf{p} - \frac{\mathbf{k}}{2}) \tag{3.25}$$

and integrate the Green function over the momentum magnitude :

$$\check{g}_{\omega_n}(\hat{\mathbf{p}}, \mathbf{k}) = \int \frac{d\xi_{\mathbf{p}}}{\pi i} \check{G}_{\omega_n}(\mathbf{p} + \frac{\mathbf{k}}{2}, \mathbf{p} - \frac{\mathbf{k}}{2}) \tag{3.26}$$

where the integration is performed over $\xi_p = p^2/2m - \mu$ near the Fermi surface and $\hat{\mathbf{p}}$ is a unit vector in the direction of $\mathbf{p}$. $\check{g}$ is called the "quasiclassical Green function". The integration over the magnitude of the momentum excludes the fast oscillations of the Green function. In the coordinate representation, we only keep the slow dependence on the center of mass coordinate ($\frac{\mathbf{r}_1+\mathbf{r}_2}{2}$) and exclude fast oscillations on the relative coordinates ($\frac{\mathbf{r}_1-\mathbf{r}_2}{2}$).

3.4.1 Eilenberger equations

The equation for the quasiclassical Green function can be derived from the Gor'kov equation (3.22). In the momentum representation we have [1]:

$$\mathbf{v}_F \mathbf{k} \check{g} - i\omega_n(\check{\tau}_3 \check{g} - \check{g}\check{\tau}_3) + \left[\check{H} * \check{g}\right] - \left[\check{g} * \check{H}\right] = \check{I} \tag{3.27}$$

The square bracket denotes the ususal convolution product in the Fourier representation and the collision integral $\check{I}$ is given by:

$$\check{I} = \left[\check{\Sigma} * \check{g}\right] - \left[\check{g} * \check{\Sigma}\right] \tag{3.28}$$

It is useful to introduce a mixed Fourier-coordinate representation to get rid of the convolution products in the Eilenberger equation (3.27):

$$\check{g}_{\omega_n}(\hat{\mathbf{p}}, \mathbf{r}) = \int \frac{d^3k}{(2\pi)^3} e^{i\mathbf{k}\mathbf{r}} \check{g}_{\omega_n}(\hat{\mathbf{p}}, \mathbf{k}) \tag{3.29}$$

Finally, it is important to notice that the quasiclassical Green function $\check{g}$ satisfies:

$$\check{g}\check{g} = \check{1} \tag{3.30}$$

The off-diagonal part of this relation is related to the particle-hole symmetry (at equilibrium) of the theory

$$g + \bar{g} = 0 \tag{3.31}$$

and the diagonal part is the so-called normalisation condition

$$g^2 - ff^\dagger = 1. \tag{3.32}$$

The components g and f of the quasiclassical matrix Green function $\check{g}$ are defined according (3.4).

3.4.2 Usadel equations

In the diffusive ("dirty") limit ($\frac{1}{\tau_e} \gg T_c$), it is possible to introduce a further simplification to the Green function formalism. In dirty superconductors, strong scattering produces averaging over momentum directions: the quasiclassical Green function $\check{g}(\hat{\mathbf{p}}, \mathbf{r})$ becomes isotropic. Therefore, we can expand it in a spherical part $\check{g}_o$ and a first order correction $\check{\mathbf{g}}$ (expansion in spherical harmonics)

$$\begin{aligned} \check{g} &= \check{g}_o + \mathbf{v_F}\check{\mathbf{g}} \\ \check{g}_o &= \langle \check{g} \rangle = \int \frac{d\Omega_p}{4\pi}\, \check{g}(\hat{\mathbf{p}}, \mathbf{r}). \end{aligned} \tag{3.33}$$

Averaging the Eilenberger equation over momentum direction, one gets:

$$D\nabla(\check{g}_o \nabla \check{g}_o) - i[\check{h}, \check{g}_o] = 0 \tag{3.34}$$

$$\check{\mathbf{g}} = -l_e g_0 \nabla g_0 \tag{3.35}$$

with

$$\check{h} = \begin{pmatrix} -i\omega_n & -\Delta \\ \Delta^\star & i\omega_n \end{pmatrix} \tag{3.36}$$

and $[.,.]$ represents a commutator. It is important to notice that the collision integral $\check{I}$ which was introduced with the Eilenberger equation vanishes after averaging over momentum direction only if there is no spin-flip or inelastic scattering. Spin-flip and electron-phonon self-energies will be discussed later.
The normalisation condition (3.30) gives:

$$\begin{aligned} \check{g}\check{g} &= \check{1} \\ \Rightarrow \check{g}_o\check{g}_o = \check{1} \quad &\text{and} \quad \check{\mathbf{g}}\check{g}_o + \check{g}_o\check{\mathbf{g}} = 0 \end{aligned} \tag{3.37}$$

The local density of state (per one spin projection) is related to the quasiclassical retarded and advanced Green functions:

$$\nu_\epsilon = \frac{1}{2}\nu_0 \left[g_o^R(\mathbf{r},\epsilon) - g_o^A(\mathbf{r},\epsilon)\right] \tag{3.38}$$

It is usefull to introduce the proximity angle θ to parameterize the Green function. The following parametrization is compatible with the normalization condition (3.37):

$$\check{g}_o^R(\epsilon) = \begin{pmatrix} \cos(\theta(\mathbf{r},\epsilon)) & -i\sin(\theta(\mathbf{r},\epsilon))e^{i\chi} \\ i\sin(\theta(\mathbf{r},\epsilon))e^{-i\chi} & -\cos(\theta(\mathbf{r},\epsilon)) \end{pmatrix} \tag{3.39}$$

and

$$\check{g}_o^A(\epsilon) = -\overline{\check{g}_o^R}(\epsilon) = \begin{pmatrix} -\cos(\overline{\theta}(\mathbf{r},\epsilon)) & -i\sin(\overline{\theta}(\mathbf{r},\epsilon))e^{i\chi} \\ i\sin(\overline{\theta}(\mathbf{r},\epsilon))e^{-i\chi} & \cos(\overline{\theta}(\mathbf{r},\epsilon)) \end{pmatrix} \tag{3.40}$$

Thus, the local density of states (DoS) per one spin projection becomes

$$\nu_\epsilon = \nu_0 \Re\cos(\theta), \tag{3.41}$$

where we use $\Re$ and $\Im$ to denote the real, respectively the imaginary part.

The formalism we derived until now can be generalised to include superconductors in a finite magnetic field. The magnetic field is taken into account by the substitution:

$$\mathbf{p} \to \mathbf{p} - \frac{e}{c}\mathbf{A}. \tag{3.42}$$

One can show [1] that the Usadel equations (3.34) have to be modified by replacing

$$\nabla \to \hat{\nabla}, \tag{3.43}$$

where the gradient operator $\hat{\nabla}$ is defined by

$$\hat{\nabla}\check{g} = \begin{pmatrix} \nabla g & \left(\nabla - \frac{2ie}{c}\mathbf{A}\right) f \\ -\left(\nabla + \frac{2ie}{c}\mathbf{A}\right) f^\dagger & -\nabla g \end{pmatrix}. \tag{3.44}$$

3.5 Spin-flip scattering

Here, we introduce scattering by impurity atoms having a finite magnetic moment as a generalisation of the scattering theory we developed in section (3.3). The theory of superconducting alloys with paramagnetic impurities was initially derived by Abrikosov and Gor'kov in [4]. Magnetic impurities introduce an exchange term in the scattering potential u. We write

$$u(\mathbf{r}-\mathbf{r}_a) = v(\mathbf{r}-\mathbf{r}_a) + v'(\mathbf{r}-\mathbf{r}_a)\mathbf{S}\frac{\hat{\sigma}}{2}, \tag{3.45}$$

where $\mathbf{S}$ is the moment of the imputity, $\frac{\hat{\sigma}}{2}$ are the electron spin matrices and $\mathbf{r}_a$ is the position of the impurity. We will assume that the spins of the impurities are oriented arbitrarily and that there is no correlation between them. Therefore it is possible to average over their direction:

$$\bar{\mathbf{S}} = 0 \quad \text{and} \quad \overline{S_i S_j} = \frac{1}{3}S(S+1)\delta_{ij}. \tag{3.46}$$

This assumption is fully valid only for low concentration of paramagnetic impurities. If the concentration is high, the interaction between the spins may result in some magnetic ordering and therefore our averaging is inapplicable. We already noticed that the functions $G_{\alpha,\beta}$ and $F_{\alpha,\beta}$ have different spin-structures (relation (3.11) and (3.12)). Therefore, we have to consider different scattering amplitudes to compute the components of the self-energy matrix $\check{\Sigma} = \begin{pmatrix} \Sigma_1 & \Sigma_2 \\ -\Sigma_2^\dagger & \bar{\Sigma}_1 \end{pmatrix}$:

$$\Sigma_1(\mathbf{p},\mathbf{k}) = n_{imp}\int \frac{d^3p_1}{(2\pi)^3}\,|u_1(\theta)|^2\,G(\mathbf{p}_1,\mathbf{p}_1-\mathbf{k}), \tag{3.47}$$

and

$$\Sigma_2(\mathbf{p},\mathbf{k}) = n_{imp}\int \frac{d^3p_1}{(2\pi)^3}\,|u_2(\theta)|^2\,F(\mathbf{p}_1,\mathbf{p}_1-\mathbf{k}), \tag{3.48}$$

with $\theta = \angle(\mathbf{p},\mathbf{p}_1)$.
Using relation (3.11) and (3.12), we get:

$$|u_1(\theta)|^2 = |v(\theta)|^2 + \frac{1}{4}S(S+1)|v'(\theta)|^2 \tag{3.49}$$

and for the anomalous part:

$$|u_2(\theta)|^2 = |v(\theta)|^2 - \frac{1}{4}S(S+1)|v'(\theta)|^2. \tag{3.50}$$

We can write these expressions in terms of quasiclassical Green functions (integrated over $d\xi_p$ near the Fermi surface) using

$$\int \frac{d^3p}{(2\pi)^3}\,\check{G}(\mathbf{p},\mathbf{p}-\mathbf{k}) = \nu_0\pi i\int \frac{d\Omega_{\mathbf{p}}}{4\pi}\,\check{g}(\hat{\mathbf{p}},\mathbf{k}) + \check{1}P\int \frac{p^2dp}{2\pi^2}\frac{1}{\xi_{\mathbf{p}}}. \tag{3.51}$$

Here P represents the principal part of the integral for which only the normal state Green function gives a significant contribution ($\Delta \ll E_F$). The last term is proportional to the unit matrix in the Nambu space and can be incorporated in the chemical potential. Therefore, the self-energies in terms of the quasiclassical Green functions become:

$$\Sigma_1(\hat{\mathbf{p}}, \mathbf{k}) = \frac{iv_F}{2} n_{imp} \int d\Omega_{\mathbf{p}_1}\, \sigma_1(\theta)\, g(\mathbf{p}_1, \mathbf{k}), \tag{3.52}$$

and

$$\Sigma_2(\hat{\mathbf{p}}, \mathbf{k}) = \frac{iv_F}{2} n_{imp} \int d\Omega_{\mathbf{p}_1}\, \sigma_2(\theta)\, f(\mathbf{p}_1, \mathbf{k}), \tag{3.53}$$

where we used the relation (3.20) between the scattering amplitudes $u_{1,2}$ and the corresponding cross sections $\sigma_{1,2}$ (Born approximation). Introducing

$$\sigma_{\mathbf{p}\mathbf{p}_1} = \frac{1}{2}\left[\sigma_1(\theta) + \sigma_2(\theta)\right] \text{ and } \sigma^{sf}_{\mathbf{p}\mathbf{p}_1} = \frac{1}{2}\left[\sigma_1(\theta) - \sigma_2(\theta)\right], \tag{3.54}$$

we separate the matrix self-energy $\check{\Sigma}$ into a non-magnetic and a spin-flip part:

$$\begin{aligned}\check{\Sigma}(\hat{\mathbf{p}}, \mathbf{k}) = {} & \frac{iv_F}{2} n_{imp} \int d\Omega_{\mathbf{p}_1}\, \sigma_{\mathbf{p}\mathbf{p}_1}(\theta)\, \check{g}(\mathbf{p}_1, \mathbf{k}) \\ & + \frac{iv_F}{2} n_{imp} \int d\Omega_{\mathbf{p}_1}\, \sigma^{sf}_{\mathbf{p}\mathbf{p}_1}(\theta)\, \check{\tau}_3 \check{g}(\mathbf{p}_1, \mathbf{k}) \check{\tau}_3.\end{aligned} \tag{3.55}$$

We can also write the self-energies in terms of the scattering mean free times $\tau_{1,2}$ corresponding to the cross sections $\sigma_{1,2}$ following relation (3.21) and introduce the spin-flip time τ_s corresponding to σ^{sf}:

$$\frac{2}{\tau_{sf}} = \frac{1}{\tau_1} - \frac{1}{\tau_2}. \tag{3.56}$$

Recall that in equation (3.55) $\check{\tau}_3$ refers to the usual Pauli matrix in the Nambu space. The collision integral $\check{I}$ which we introduced in the Eilenberger equation (3.27) will therefore consist in two parts. To derive the contributions of the self-energies to the Usadel equation, we have to compute their average over the direction of the momentum $\mathbf{p}$. One can show (see for e.g. [1]) that the non-magnetic part vanishes after averaging over momentum direction. The spin-flip part of the collision integral does not vanish when averaged because $\check{g}$ and $\check{\tau}_3 \check{g} \check{\tau}_3$ do not commute.

In the dirty limit, it is possible to expand the Green function in spherical harmonics. Using the expansion (3.33) to compute the collision integral and neglecting the second order terms in $\check{\mathbf{g}}$ (the vector part is expected to be smaller than the spherical part $\check{g}_o$), we get for the spin-flip part of the averaged collision integral:

$$\left\langle \check{I}^s \right\rangle = \frac{iv_F}{2} n_{imp} \int \frac{d\Omega_p}{4\pi} \left[\int d\Omega_{p'} \sigma^{sf}_{\mathbf{p},\mathbf{p}'} \check{\tau}_3 (\check{g}_o + \hat{v}'_F \check{\mathbf{g}}) \check{\tau}_3, (\check{g}_o + \hat{v}_F \check{\mathbf{g}}) \right] \tag{3.57}$$

$$= \begin{pmatrix} 0 & \frac{2i}{\tau_{sf}} g_o f_o \\ \frac{2i}{\tau_{sf}} g_o f_o^\dagger & 0 \end{pmatrix} \tag{3.58}$$

The non vanishing off-diagonal terms will introduce the effect of spin-flip scattering in the Usadel equation (3.34).

At this point, we are able to describe scattering at the level of the Usadel equations. Using the parametrisation (3.39) of the Green function and including the spin-flip term in the Usadel equations, we obtain the equation for the proximity angle $\theta(x, \epsilon)$:

$$\frac{D\partial_x^2\theta}{2} + (i\epsilon - \Gamma_{in}) \sin\theta - \left[2\Gamma_{sf} + \frac{2e^2 D A^2}{c^2}\right] \cos\theta \sin\theta + \Delta \cos\theta = 0, \tag{3.59}$$

where the spin-flip and inelastic scattering rates are defined by

$$\Gamma_{sf} = \frac{1}{2\tau_{sf}} \quad \text{and} \quad \Gamma_{in} = \frac{1}{2\tau_{in}}. \tag{3.60}$$

We included inelastic scattering as an homogeneous broadening of the energy. The physical origin of inelastic scattering is electron-phonon scattering, a smaller contribution comes from electron-electron scattering.

3.6 Pair breaking effect of a magnetic field

If an external magnetic field is applied on a superconducting material, the time reversal symmetry

$$\mathbf{p} \leftrightarrow -\mathbf{p} \tag{3.61}$$

$$\uparrow \leftrightarrow \downarrow \tag{3.62}$$

between the electrons of a Cooper pair is broken [19]. This results in the suppression of the pair amplitude in both usual and proximity superconductors.

Consider a thin S-N wire with a parallel applied magnetic field [14]. If the thickness of the wire is much smaller than the London penetration depth, it is reasonable to neglect the screening of the magnetic field. Therefore, we consider a constant magnetic field $\mathbf{H}$ parallel to the wire and write the corresponding potential

$$\mathbf{A} = \frac{r\, H\, \mathbf{u}_\varphi}{2}. \tag{3.63}$$

where we use polar coordinates $(\mathbf{u}_r, \mathbf{u}_\varphi)$. For a thin wire, we can replace A^2 in the Usadel equation (3.59) by its average over the width of the wire

$$\langle A^2 \rangle = \frac{1}{R} \frac{H^2}{4} \int_0^R r^2 dr = \frac{H^2 R^2}{12}. \tag{3.64}$$

In this case, the effect of a magnetic field can be included in equation (3.59) considering an effective spin-flip rate

$$\Gamma_{sf}^{eff} = \Gamma_{sf} + \frac{e^2 D H^2 R^2}{6c^2}. \tag{3.65}$$

A similar description can be applied to a thin S-N film (see for e.g. [7]).

4 Solution for a homogeneous superconductor

In this work, we study the effect of spin-flip and inelastic scattering on a proximity superconductor. It is important to discuss the solution of the Usadel equations for a homogeneous superconductor (with finite pairing interaction), in particular at zero-energy, to have a basis for further comparisons.

The Usadel equation (3.59) for a homogeneous superconductor reads:

$$(i\epsilon - \Gamma_{in})\sin\theta - 2\Gamma_{sf}\cos\theta\sin\theta + \Delta\cos\theta = 0 \tag{4.1}$$

Without spin-flip and inelastic scattering, we recover the BCS solution:

$$\theta(x) = \begin{cases} \frac{\pi}{2} + i\,\mathrm{arg\,tanh}(\frac{\epsilon}{\Delta}) & |\epsilon| < \Delta \\ \\ i\,\mathrm{arg\,tanh}(\frac{\Delta}{\epsilon}) & |\epsilon| > \Delta \end{cases} \tag{4.2}$$

$$\Rightarrow \nu(\epsilon) = \nu_o \frac{|\epsilon|}{\sqrt{\epsilon^2 - \Delta^2}}\,\Theta(\epsilon^2 - \Delta^2) \tag{4.3}$$

From equation (4.1), it is clear that if we consider a finite inelastic scattering rate Γ_{in}, it is not possible to find a zero-DoS solution.
Introducing only the spin-flip term, we see that it is possible to find zero-DoS solutions up to a certain energy, which depends on Γ_{sf}. This energy (Gap in the DoS) can be determined analytically [23]

$$E_g(\Gamma_{sf}) = \left[\Delta^{2/3} - (2\Gamma_{sf})^{2/3}\right]^{3/2}. \tag{4.4}$$

This is the frontier between the gaped and the gapless domain (respectively domain I and II in Figure 3). If we write

$$\Gamma_{sf} = \frac{\Delta}{2} - \delta\Gamma_{sf} = \Gamma_{sf}^c - \delta\Gamma_{sf}, \tag{4.5}$$

and measure the energies in the units of Δ (which is the only relevant scale of the system), we get the form of expression (4.4) close to Γ_{sf}^c:

$$E_g(\delta\Gamma_{sf}) = \sqrt{2}\,(\frac{4}{3}\delta\Gamma_{sf})^{3/2} \tag{4.6}$$

At zero-energy, we see from equation (4.1) that the solution

$$\theta = \frac{\pi}{2} \Rightarrow \nu = \nu_o \Re\cos\theta = 0 \tag{4.7}$$

is always valid. However, it is interesting to notice that at zero-energy, equation (4.1) has other zero-DoS solution:

$$\theta = \frac{\pi}{2} \pm i\,\mathrm{arg\,cosh}(\frac{\Delta}{2\Gamma_{sf}}) \tag{4.8}$$

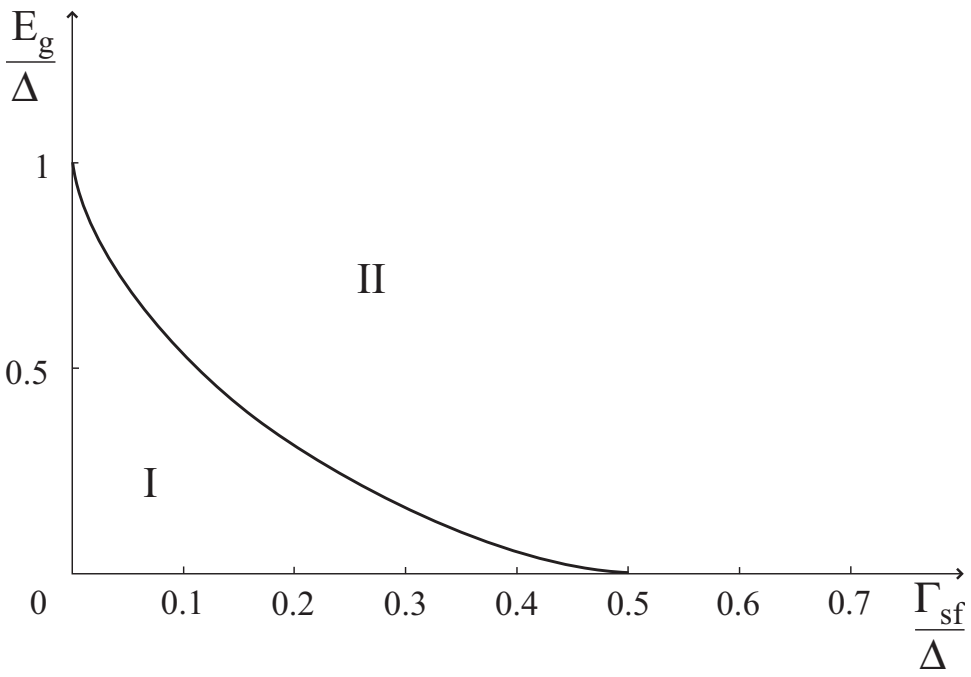

Figure 3: Gap in the DoS for a homogeneous superconductor containing magnetic impurities

These two new solutions have to be rejected because they lead to a diverging imaginary part when $\Gamma_{sf} \to 0$. The three solutions at zero-energy merge when the spin-flip rate reaches the critical value $\Gamma_{sf}^c = \frac{\Delta}{2}$. Above Γ_{sf}^c the solution (4.8) becomes

$$\theta = \frac{\pi}{2} \pm \arccos(\frac{\Delta}{2\Gamma_{sf}}), \tag{4.9}$$

where the plus sign has to be rejected because it corresponds to a negative DoS. If the spin-flip rate is increased, the solution (4.9) leads to a DoS saturating to ν_o, the normal DoS. However, this solution is not unique: the solution $\theta = \frac{\pi}{2}$ is still valid. Solving numerically equation (4.1) for finite energies and spin-flip rates above Γ_{sf}^c, we can see that only the solution saturating to the normal DoS (4.9) can be properly continued to finite energies, in the sense that it is possible to recover this solution taking a continuous path in the gapless domain (domain II in Figure 3) from the $\Gamma_{sf} = 0$ BCS solution above the gap.

5 Usadel equations for the S-N system

5.1 Boundary conditions for the S-N system

We must now introduce appropriate boundary conditions to include an hybrid structure in our description. The boundary conditions for the Usadel equation were derived in [10] for arbitrary interface transparency. We will restrict ourselves to the case of a transparent interface. The boundary conditions at the S-N interface ($x = 0$) described in section (2.3) are:

- transparency: $g_o(0-) = g_o(0+)$ (5.1)
- conservation of the current: $\sigma_s g_o \partial_x g_o(0-) = \sigma_n g_o \partial_x g_o(0+)$ (5.2)

where $\sigma_{s,n}$ are the metallic conductances on both sides of the S-N interface. For the boundary $x = -\infty$ we have:

$$\theta(x = -\infty) = \theta_s \tag{5.3}$$

where θ_s is the value of the proximity angle in the bulk superconductor. At $x = L$ (interface with vacuum), the conservation of the quasiparticle current yields:

$$\partial_x \theta(x = L) = 0 \tag{5.4}$$

To simplify the model, we will also use a rigid boundary at the S-N interface: we will take the zero-energy bulk value ($\theta = \frac{\pi}{2}$) for the proximity angle at $x = 0$. This rigid boundary condition is fully justified if the normal part is much more disordered than the superconducting part or if the gap Δ in the S-part is much larger than the Thouless energy of the N-part E_{Th} (for more details see Appendix B and the discussion of the boundary in section (8)).

The relevant energy and length scales in our system are the Thouless energy E_{Th} and the length L of the N-part. Therefore, in the following discussion we will consider a sample of length $L = 1$ and measure the energies in units of E_{Th}, except in section (8), where we go beyond the rigid boundary and have to reintroduce the diffusion constants in the Usadel equations.

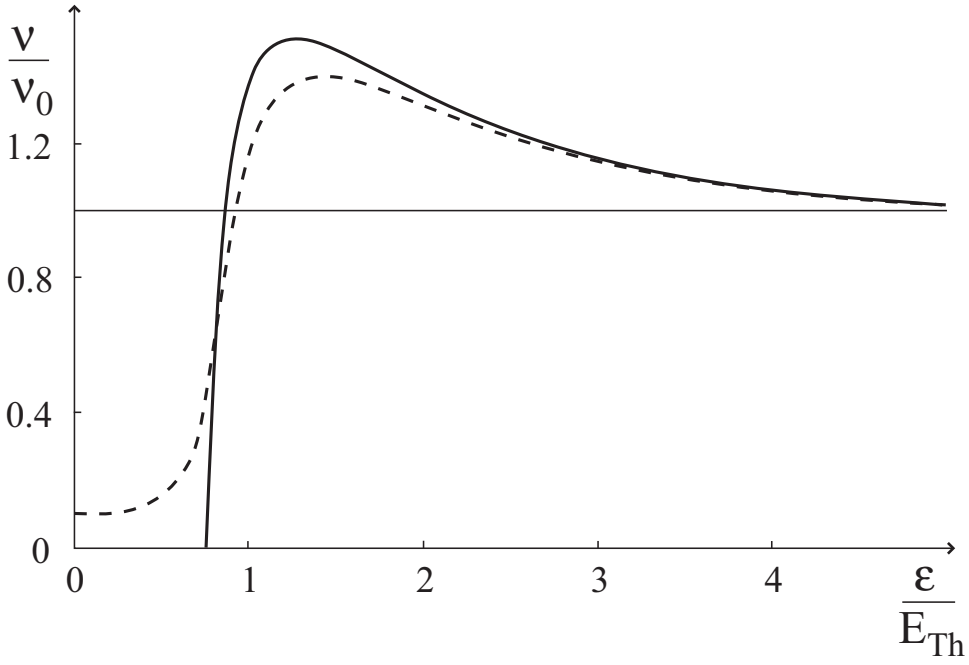

Figure 4: Minigap in the local density of states (x=1) of the N-part for $\Gamma_{in} = 0$ (solid line) and $\Gamma_{in} = 0.1\, E_{Th}$ (dashed line).

5.2 Minigap in the DoS of the N-part

The analytical solution of the Usadel equation (3.59) in the absence of pair breaking and inelastic scattering has been discussed in [7] for infinite length junctions and in [6] for thin N-layers. In appendix B, we briefly review these solutions. The most striking feature of S-N systems is the apparition of a gap ("minigap") of the order of the Thouless energy E_{Th} in the N-part of the junction. If we consider an infinite system, the Thouless energy (2.14) is zero and the minigap in the DoS vanishes. The solution for the finite size S-N system can be written in terms of Jacobi elliptic functions and leads to the LDoS represented in figure (4).

6 Linearization of the Usadel equations

The Usadel equations are highly nonlinear equations. However, certain properties of the solution can be obtained from the linearised equations. For example, the reentrance effect [5] is already present in the linear approximation. We have to keep in mind that this is a rough approximation and that therefore we will loose important features of the system: this approximation is not sufficient to get information on the size of the minigap ($\sim E_{Th}$) in the density of state of the N-part.

6.1 Linearization close to $\theta = \frac{\pi}{2}$

In the absence of spin-flip and inelastic scattering, the zero-energy solution of the Usadel equation (3.59) for the S-N system is $\theta(x) = \frac{\pi}{2}$ over the whole junction. For small scattering rates and energy, we expect that the deviation over this value is small. We write the finite energy and scattering rate solution $\theta = \frac{\pi}{2} + \delta\theta_1 + i\delta\theta_2$ and take into account only the linear terms in $\delta\theta_{1,2}$. Separating the real and the imaginary part of the Usadel equation and measuring the energies in the units of E_{Th}, we get:

$$\begin{cases} \partial_x^2 \delta\theta_1 = 2\Gamma_{in} - 4\Gamma_{sf}\delta\theta_1 \\ \partial_x^2 \delta\theta_2 = -2\epsilon - 4\Gamma_{sf}\delta\theta_2 \end{cases} \tag{6.1}$$

These equations are supplied with the boundary conditions (5.2) and (5.2) for $\delta\theta_{1,2}$:

$$\text{rigid boundary} \Rightarrow \delta\theta_{1,2}|_{x=0} = 0 \tag{6.2}$$

$$\text{interface with vacuum} \Rightarrow \partial_x \delta\theta_{1,2}|_{x=1} = 0 \tag{6.3}$$

First, we can notice that the real and the imaginary part are not coupled and therefore, we can treat them separately. Without spin-flip, the solution of (6.1) is:

$$\begin{cases} \delta\theta_1 = -\Gamma_{in} x(2-x) \\ \delta\theta_2 = \epsilon\, x(2-x) \end{cases} \tag{6.4}$$

In figure 5, we compare this result with the exact solution of appendix B at zero-energy. Introducing spin-flip, this solution becomes:

$$\begin{cases} \delta\theta_1 = -\frac{\Gamma_{in}}{2\,\Gamma_{sf}\cos(2\sqrt{\Gamma_{sf}})}\left[\cos(2\sqrt{\Gamma_{sf}}(x-1)) - \cos(2\sqrt{\Gamma_{sf}})\right] \\ \delta\theta_2 = \quad \frac{\epsilon}{2\,\Gamma_{sf}\cos(2\sqrt{\Gamma_{sf}})}\left[\cos(2\sqrt{\Gamma_{sf}}(x-1)) - \cos(2\sqrt{\Gamma_{sf}})\right] \end{cases} \tag{6.5}$$

To the linear order, the local density of states (LDoS) is given by:

$$\nu(x) = \nu_0 \overbrace{\cos(\frac{\pi}{2} + \delta\theta_1)\cosh\delta\theta_2}^{\Re\cos\theta} \cong -\nu_0\,\delta\theta_1 \tag{6.6}$$

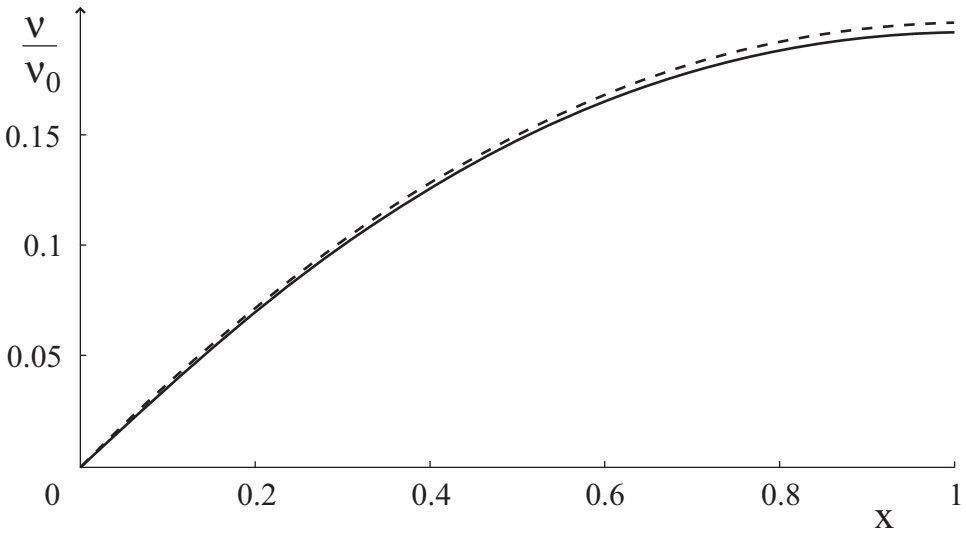

Figure 5: LDoS in the N-part: comparison between the linearised (dash) and the exact solution (solid) for $\Gamma_{in} = 0.2\, E_{Th}$.

From equation (6.5), we can see that if $\Gamma_{in} = 0$, the density of states in the linear approximation is zero.

Now we consider small spin-flip rates Γ_{sf} and expand the solution (6.5) to the leading (linear) order in Γ_{sf}:

$$\begin{cases} \delta\theta_1 \cong -\Gamma_{in}(1 + 2\Gamma_{sf})x(2 - x) \\ \delta\theta_2 \cong \quad \epsilon(1 + 2\Gamma_{sf})x(2 - x) \end{cases} \tag{6.7}$$

These equations are similar to (6.4) and suggest to introduce:

$$\Gamma^{\star}_{in} = \Gamma_{in}(1 + 2\Gamma_{sf}) \quad \text{and} \quad \epsilon^{\star} = \epsilon\,(1 + 2\Gamma_{sf}) \tag{6.8}$$

For a small Γ_{sf}, the correction of spin-flip scattering on the DoS can be reduced to an "effective" inelastic scattering rate $\Gamma^{\star}_{in}$.

The solution of the linearised equations (6.5) is usefull to get an idea on the local density of states in the junction. We can also see that this approximation is too crude to access to the dependence on energy of the density of states. In the linear approximation, the DoS is given by (6.6) and does not depend on energy. Therefore the linearization close to the rigid boundary can only be used to get information on the presence of a finite subgap density of states when small inelastic and spin-flip scattering are present.

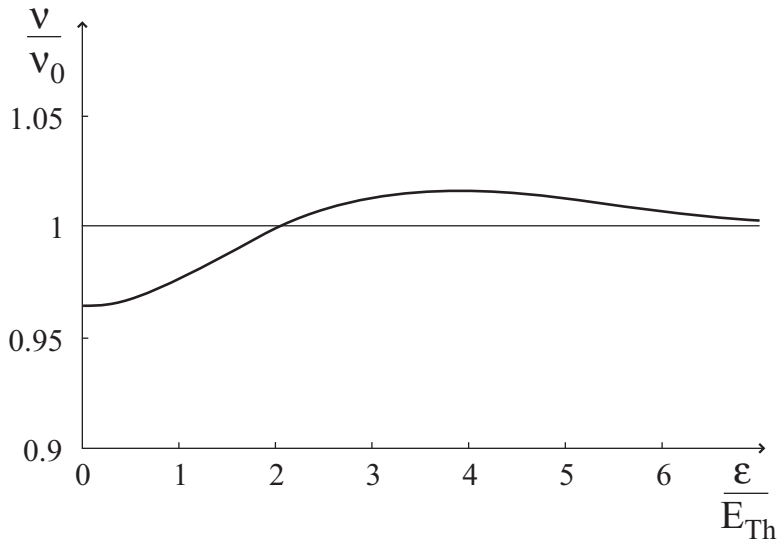

Figure 6: LDoS at $x = 1$ for $\Gamma_{sf} = 1.5\, E_{Th}$

6.2 Linearization close to $\theta = 0$

In the following sections, we will see that for large spin-flip scattering rates, the density of states in the normal part of the junction saturates to the normal density of states ν_o everywhere except in a restricted domain close to the rigid boundary $\theta = \frac{\pi}{2}$. Therefore, another way to linearise the equations is to expand close to $\theta = \delta\theta \approx 0$. The Usadel equation (3.59) becomes:

$$\frac{\partial_x^2 \delta\theta}{2} + (i\epsilon - \Gamma_{in})\delta\theta - 2\Gamma_{sf}\delta\theta = 0 \tag{6.9}$$

$$\Rightarrow \partial_x^2 \delta\theta = \alpha\, \delta\theta \tag{6.10}$$

with

$$\alpha = 4\Gamma_{sf} - 2(i\epsilon - \Gamma_{in}) \tag{6.11}$$

The solution of equation (6.10) satisfying the boundary conditions (6.2) and (6.3) is:

$$\delta\theta = \frac{\pi}{2}\, \frac{1}{1 + e^{-2\sqrt{\alpha}}} \left[e^{-\sqrt{\alpha}x} + e^{\sqrt{\alpha}(x-2)} \right] \tag{6.12}$$

In figure 6, we represent the LDoS at $x = 1$ as a function of the energy. We have chosen a large spin-flip rate $\Gamma_{in} = 1.5\, E_{Th}$ where the zero-energy value of the density of states is close to the exact value we will find in section (8). From this comparison with the exact zero-energy value, we see that the expansion clearly fails for smaller spin-flip rates.

7 First integral

The aim of this section is to discuss the presence of zero-DoS solutions working with the first integral of equation (3.59). Here, we show that the effect of spin-flip scattering on the density of states of a proximity superconductor is very similar to its effect on a homogeneous superconductor, which has been discussed in section (4). We observe in particular:

- a minigap E_g (dependent on the magnitude of the spin-flip rate) in the DoS of the N-part,
- a critical spin-flip rate Γ_{sf}^c where this minigap closes.

The relevant scale for E_g and Γ_{sf}^c will be the Thouless energy E_{Th} of the N-part instead of the superconducting gap Δ.

The Usadel equation (3.59) for the N-part of the junction can be integrated once yielding:

$$\frac{1}{4}(\partial_x\theta)^2 - (i\epsilon - \Gamma_{in})\cos\theta + \Gamma_{sf}\cos^2\theta = C(\epsilon). \tag{7.1}$$

We consider again a N-part of length unity and write the energies in units of E_{Th}. The constant in the r.h.s. can be obtained from the boundary condition at the interface with vacuum (5.4):

$$C(\epsilon) = -(i\epsilon - \Gamma_{in})\cos\theta^1 + 2\Gamma_{sf}\cos^2\theta^1, \tag{7.2}$$

where we use the notation $\theta(x = 0, 1) = \theta^{0,1}$. At the S-N interface, we keep using the rigid boundary $\theta^0 = \frac{\pi}{2}$.

7.1 Gap solution

First, we try to find zero-DoS solutions for the Usadel equation (solution in the minigap)

$$\nu(x, \epsilon) = 0 \Leftrightarrow \Re(\theta) = \frac{\pi}{2}. \tag{7.3}$$

Therefore, we write $\theta = \frac{\pi}{2} + i\Theta$ with Θ real. Then we separate the real and the imaginary part of (7.1):

$$\begin{cases} \frac{1}{4}(\partial_x\Theta)^2 - \epsilon\sinh\Theta - \Gamma_{sf}\sinh^2\Theta = \Re(C) \\ -\Gamma_{in}\sinh\Theta = \Im(C) \end{cases} \tag{7.4}$$

From the imaginary part, we can see that if Γ_{in} is finite, it is not possible to find a zero-DoS solution. Indeed, the imaginary part of (7.4) gives

$$\Theta(x) = \Theta^0 \quad \forall x \in [0, 1], \tag{7.5}$$

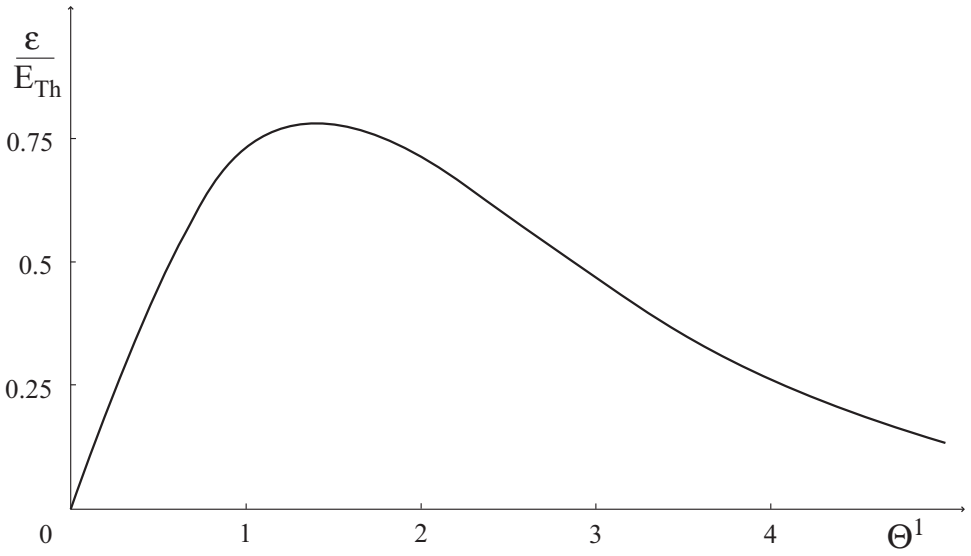

Figure 7: Second integral of the Usadel equation for $\Gamma_{sf} = 0$

which is not a solution of the Usadel equation (3.59).

In the following, we set $\Gamma_{in} = 0$ and continue to search for zero-DoS solutions. In the absence of inelastic scattering, equation (7.4) becomes:

$$\partial_x \Theta = 2\sqrt{\epsilon}\left[\left(\sinh\Theta^1 - \sinh\Theta\right) + \frac{\Gamma_{sf}}{\epsilon}\left(\sinh^2\Theta^1 - \sinh^2\Theta\right)\right]^{1/2}. \quad (7.6)$$

Then we integrate both sides of this equation over the junction:

$$\sqrt{\epsilon} = \int_0^{\Theta^1} \frac{d\Theta}{2\left[\left(\sinh\Theta^1 - \sinh\Theta\right) + \frac{\Gamma_{sf}}{\epsilon}\left(\sinh^2\Theta^1 - \sinh^2\Theta\right)\right]^{1/2}}. \quad (7.7)$$

The minigap E_g is the maximal energy compatible with a zero-DoS solution. Without spin-flip, this is the well known result [8]:

$$E_g^0 = \max_{\Theta^1}\left[\int_0^{\Theta^1} \frac{d\Theta}{2\left(\sinh\Theta^1 - \sinh\Theta\right)^{1/2}}\right]^2. \quad (7.8)$$

In Figure 7, we have plotted the energy as a function of Θ^1 using equation (7.7) with $\Gamma_{sf} = 0$. We can see that for a finite energy, we have two possible values for the proximity angle at the boundary Θ^1. At zero energy, the second branch leads to a diverging Θ^1 and therefore we reject this solution. This continuity argument is commonly accepted in the quasiclassical approximation, but the second solution may play an important role

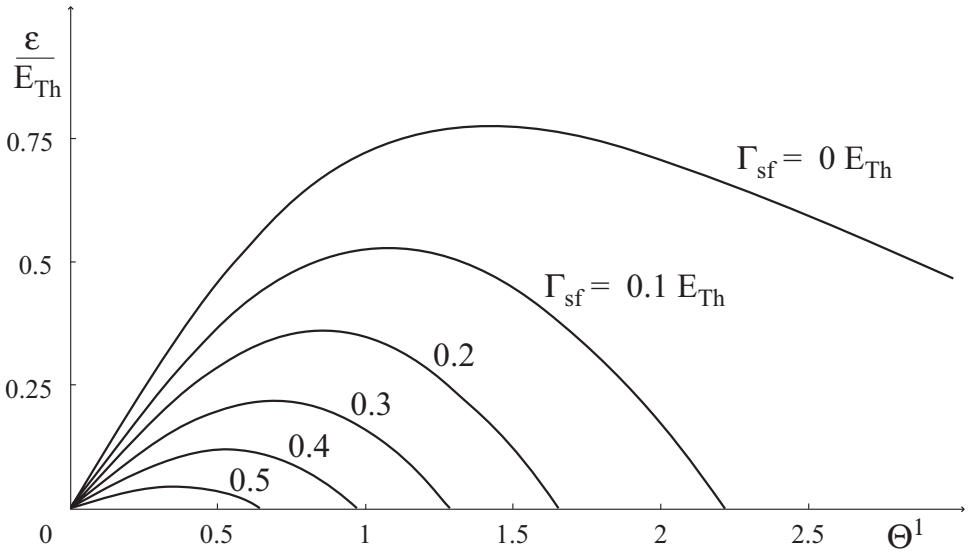

Figure 8: Second integral for $\Gamma_{sf} = 0$ (upper curve), 0.1, 0.2, 0.3, 0.4 and 0.5 E_{Th}

in models including mesoscopic fluctuations [13]. The maximum energy is obtained for $\hat{\Theta}^1 \approx 1.421$ which corresponds to an energy $E_g^0 \approx 0.78\, E_{Th}$. It is important to notice that the result we get here for the S-N junction differs from the result obtained in [8] for the S-N-S junction by a factor 4: a S-N-S junction of length 1 without phase difference is equivalent to a S-N junction of length $\frac{1}{2}$) and therefore, we work with a different energy scale E_{Th}. All the results we give here for the density of states at the interface with vacuum in a S-N junction also describe the density of states in the middle of a S-N-S junction with the superconducting terminals having the same phase.

Now, we discuss expression (7.7) for $\Gamma_{sf} \neq 0$. If a finite spin-flip rate is introduced, the second branch of the solution no longer diverges at zero energy (Figure 8). However, this new zero-energy solution is not acceptable in our model because of its behaviour when $\Gamma_{sf} \to 0$: without spin-flip we recover the situation of Figure 7 with a second branch diverging at zero energy.

If spin-flip is increased up to a critical rate Γ_{sf}^c, the two solutions at zero energy merge and the gap closes. From equation (7.7), it is possible to find this Γ_{sf}^c. Indeed, close to Γ_{sf}^c, the value of the proximity angle at the boundary with vacuum Θ^1 corresponding to the second zero-energy solution

is expected to be small. At zero-energy, equation (7.7) becomes :

$$\Gamma_{sf} = \left[\int_0^{\Theta^1} \frac{d\Theta}{2\left(\sinh^2\Theta^1 - \sinh^2\Theta\right)^{\frac{1}{2}}} \right]^2 \tag{7.9}$$

The closing point corresponds to the limit $\Theta_1 \to 0$ of this integral. Expanding the integrand, we get :

$$\lim_{\Theta^1 \to 0} \left[\int_0^{\Theta^1} \frac{d\Theta}{2\left(\Theta^{1\,2} - \Theta^2\right)^{\frac{1}{2}}} \right]^2 = \frac{\pi^2}{16} \tag{7.10}$$

$$\Rightarrow \Gamma_{sf}^c \approx 0.62\, E_{Th} \tag{7.11}$$

7.2 Zero-energy gapless solution

Using the method of the first integral it is possible to find a finite DoS solution even at zero-energy. This solution is valid for Γ_{sf} larger than the critical value of the spin-flip rate Γ_{sf}^c at which the minigap closes. It corresponds to purely real values of the proximity angle, therefore we write $\theta = \frac{\pi}{2} + \beta$, with β real. The first integral of the Usadel equation becomes:

$$\frac{1}{4}(\partial_x \beta)^2 + \Gamma_{sf} \sin^2\beta = C, \tag{7.12}$$

where

$$C = \Gamma_{sf} \sin^2\beta^1. \tag{7.13}$$

Integrating this equation over the junction, we get

$$\Gamma_{sf} = \left[\int_0^{\beta^1} \frac{d\beta}{2\left(\sin^2\beta^1 - \sin^2\beta\right)^{\frac{1}{2}}} \right]^2. \tag{7.14}$$

This solution leads to a DoS saturating to unity (in the units of the normal state DoS ν_o) as Γ_{sf} is increased. In Figure 9, we see that only the left branch of the graph leads to a positive DoS. Indeed, we have

$$\nu(\epsilon) = \nu_o \cos\theta = -\nu_o \sin\beta. \tag{7.15}$$

The asymptotics for large spin-flip rates of the left branch of the curve is $\beta = -\frac{\pi}{2}$ wich corresponds to $\nu(\epsilon) = \nu_o$, the DoS in the normal state. In section (8), we will find the density of states close to the critical spin-flip rate using a general zero-energy solution in terms of Jacobi elliptic functions.

The constant solution $\theta = \frac{\pi}{2} \Rightarrow \beta = 0$ is always present at zero-energy. As we did for the solution in the gap, we need to discuss which solution we

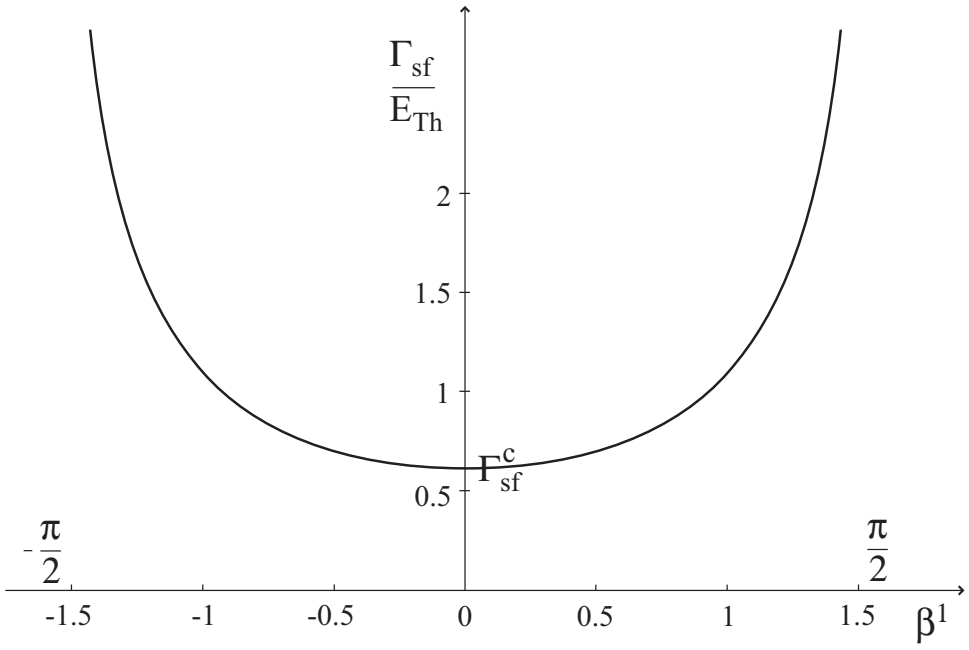

Figure 9: Zero-energy gapless solution: Γ_{sf} v.s β^1

have to keep. To achieve this goal, let's apply again the method of the first integral (but this time we have to consider a complex θ^1), we get:

$$\int_{\frac{\pi}{2}}^{\theta^1} \frac{d\theta}{2\left[i\epsilon\left(\cos\theta^1-\cos\theta\right)-\Gamma_{sf}\left(\cos^2\theta^1-\cos^2\theta\right)\right]^{1/2}}=1. \tag{7.16}$$

To compute the integral in the l.h.s. as a function of the complex parameter θ^1, we notice that the integrand has no poles in the half plane $\Re\cos\theta>0$ (physical DoS). We choose an explicit path to compute numerically the integral and plot the real and the imaginary part of this integral as a function of the complex θ^1. Equation (7.16) is solved for the values of θ^1 where the imaginary part of the integral vanishes and the real part equals one. The argument is the same as the one we used for the homogeneous superconductor in section 4: we take a path in the gapless regime and see which solution can be continued to the zero spin-flip gapless solution. It turns out that the solution $\theta=\frac{\pi}{2}$ acquires a diverging imaginary part along the path we choose and therefore cannot be properly continued to the zero spin-flip solution.

7.3 Dependance of the minigap on Γ_{sf}

7.3.1 Small Γ_{sf} limit

If we consider a finite but small spin-flip rate Γ_{sf}, we can get a correction to the value of the minigap E_g^0. We write equation (7.7):

$$2\sqrt{\epsilon} = \int_0^{\Theta^1} \frac{1}{[\sinh\Theta^1 - \sinh\Theta]^{1/2}} \cdot \frac{1}{\left[1 + \frac{\Gamma_{sf}}{\epsilon}\left(\sinh\Theta^1 + \sinh\Theta\right)\right]^{1/2}} d\Theta \tag{7.17}$$

and expand the integrand in the small parameter $\frac{\Gamma_{sf}}{\epsilon}\left(\sinh\Theta^1 + \sinh\Theta\right) < 2\,\frac{\Gamma_{sf}}{\epsilon}\sinh\Theta^1$. Taking into account that $\Theta^1 \approx 1.421$ and $\epsilon \approx E_g^0$, we can see that this expansion loses its validity for $\Gamma_{sf} \sim 0.1\,E_{Th}$.
The resulting correction to the minigap is:

$$E_g \approx \left(C_1 - C_2\Gamma_{sf}\right), \tag{7.18}$$

where the coefficients are given by:

$$C_1 = E_g^0 \tag{7.19}$$

$$C_2 = \frac{\int_0^{\hat{\Theta}^1} \frac{\left(\sinh\Theta^1 + \sinh\Theta\right)}{(\sinh\Theta^1 - \sinh\Theta)^{1/2}} d\Theta}{\int_0^{\hat{\Theta}^1} \frac{d\Theta}{(\sinh\Theta^1 - \sinh\Theta)^{1/2}}} \approx 3.09 \tag{7.20}$$

From the magnitude of the coefficent C_2, we can see that even a small spin-flip rate strongly affects E_g.

7.3.2 Gap curve close to Γ_{sf}^c

Close to Γ_{sf}^c, it is not sufficient to expand directly equation (7.7) in the small variation on the critical value $\Gamma_{sf} = \Gamma_{sf}^c - \delta\Gamma_{sf}$. The problem is that close to the critical spin-flip rate, the energy and the value of $\sinh\Theta^1$ are also small. Therefore, it is necessary to get a more accurate expression in $\delta\Gamma_{sf}$. From equation (7.7), we have

$$2\sqrt{\Gamma_{sf}} = \int_0^{\Theta^1} \frac{1}{\left[\left(\sinh^2\Theta^1 - \sinh^2\Theta\right) + \frac{\epsilon}{\Gamma_{sf}}\left(\sinh\Theta^1 - \sinh\Theta\right)\right]^{1/2}} d\Theta. \tag{7.21}$$

The minigap $E_g(\Gamma_{sf})$ corresponds to the maximal energy compatible with a zero DoS solution (real Θ). In appendix C, we study the dependance of the minigap on the spin-flip rate near the closing point. As a result, we get

$$E_g = 2\left(\frac{2}{3}\right)^{3/2}\left[\delta\Gamma_{sf}\right]^{3/2} \tag{7.22}$$

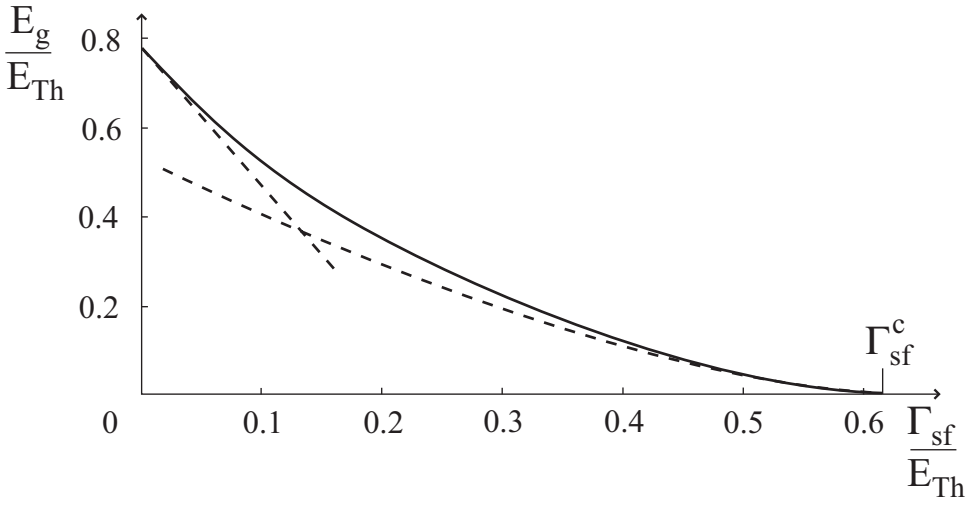

Figure 10: Numerical gap curve (solid line): comparison with asymptotic expressions (dashed lines)

Close to the critical spin-flip rate, the minigap curve is slower than linear in $\delta\Gamma_{sf}$. It is interesting to notice that we find the same power law as in the discussion for the homogeneous superconductor, relation (7.22) can be compared with (4.6).

7.3.3 Numerical gap curve

To get the complete gap curve $E_g(\Gamma_{sf})$, we have to solve the implicit integral equation (7.21). This equation is equivalent (see appendix C) to:

$$\int_0^{x_1} \frac{1}{\sqrt{\Gamma_{sf}\left(x_1^2 - x^2\right) + \epsilon\,(x_1 - x)}} \cdot \frac{1}{\sqrt{1+x^2}} dx = 2. \tag{7.23}$$

The integral in the l.h.s. is elliptic and (7.23) can be written in the form:

$$A \cdot F(\phi, k) = 2, \tag{7.24}$$

where F is the incomplete elliptic integral of the first kind:

$$F(\phi, k) = \int_0^{\phi} \frac{d\varphi}{\sqrt{1 - k^2 \sin^2 \varphi}}. \tag{7.25}$$

A, ϕ and k are functions of the variables Γ_{sf}, ϵ and x_1. For a fixed value of Γ_{sf}, the minigap E_g is the maximal energy compatible with a real x_1. Solving numerically equation (7.24), we get the gap curve represented in Figure 10.

8 Zero-energy solution for finite Γ_{sf}

In this section, we consider an S-N junction at zero-energy with the following simplifications:

- we introduce a finite spin-flip rate Γ_{sf} only in the N-part
- we neglect self-consistency in the S-part.

The Usadel equations for the S-, respectively the N-part of the junction read:

$$\frac{1}{2}D_s\partial_x^2\theta + \Delta\cos\theta = 0 \tag{8.1}$$

$$\frac{1}{2}D_n\partial_x^2\theta - 2\Gamma_{sf}\cos\theta\sin\theta = 0 \tag{8.2}$$

Here, we have reintroduced the diffusion constants $D_{n,s}$ in the Usadel equations because they may take different values in the S- and the N-part. These equations are supplied with the boundary conditions described in section (5.1) at $x = 0$ (S-N interface) and $x = 1$ (interface with vacuum). The boundary condition at $x = -\infty$ is $\theta = \theta^s$, the bulk solution which is $\pi/2$ at zero-energy.

First, we write the solutions of (8.1) and (8.2) in terms of the parameters $\theta(x = 0, 1) = \theta^{0,1}$ to be determined later using the boundary condition at the S-N interface. The solution for the semi-infinite S-part is given in [7]:

$$\theta(x) = \theta^s + 4\arctan\left[\tan\left(\frac{\theta^0 - \theta^s}{4}\right)\exp\left(\sqrt{\frac{2\Delta}{D_s}}\,x\right)\right] \tag{8.3}$$

$$x \to -\infty \quad \Rightarrow \quad \theta \to \theta^s = \frac{\pi}{2} \tag{8.4}$$

$$x \to 0 \quad \Rightarrow \quad \theta \to \theta^0 \tag{8.5}$$

For the N-part, we found a solution in terms of Jacobi elliptic functions (see Appendix A for the complete derivation):

$$\theta(x) = \arcsin\left[\sin\theta^1\mathrm{dn}^{-1}\left(2\sqrt{\frac{\Gamma_{sf}}{D_n}}(x-1), \cos\theta^1\right)\right] \tag{8.6}$$

The interface transparency ($\theta(0^-) = \theta(0^+)$) gives:

$$\sin\theta^0 = \sin\theta^1\mathrm{dn}^{-1}[-2\sqrt{\frac{\Gamma_{sf}}{D_n}}, \cos\theta^1] \tag{8.7}$$

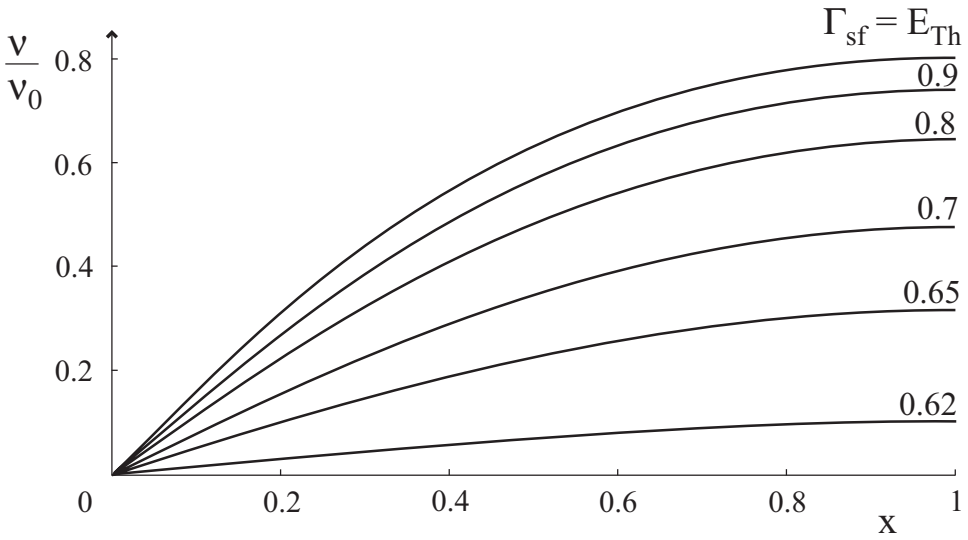

Figure 11: Local density of states in the N-part at zero energy for $\Gamma_{sf} = 0.62 - 1\, E_{Th}$.

And the conservation of the quasiparticle current yields (see Appendix A for the details):

$$\sin(\frac{\theta^0 - \theta^s}{2}) = \gamma\sqrt{\frac{\Gamma_{sf}}{2\Delta}}\sqrt{\sin^2\theta^0 - \sin^2\theta^1} \tag{8.8}$$

where $\gamma = \frac{\sigma_n/\sigma_s}{\sqrt{D_n/D_s}}$. Solving numerically (8.7) and (8.8), one gets the values of the proximity angle $\theta^{0,1}$ at the boundaries. In figure 11, we have represented the LDoS in the N-part of the junction for various spin-flip rates using this solution.

We can see from (8.8) that it is justified to use the rigid boundary condition $\theta^0 = \frac{\pi}{2}$ if $\Gamma_{sf} \ll \Delta$ or if the N-part is much more disordered than the S-part (the metallic conductivity σ is proportional to the diffusion constant)

$$D_n \ll D_s \Rightarrow \gamma \ll 1. \tag{8.9}$$

The solution we have presented here allows to find the critical Γ_{sf} (closing of the gap) and to get an analytical expression for the DoS near this critical point. Using the rigid condition for θ^0, the boundary (8.7) becomes (for Γ_{sf} given in the units of E_{Th}):

$$\sin\theta^1 = \mathrm{dn}[-2\sqrt{\Gamma_{sf}}, \cos\theta^1] \tag{8.10}$$

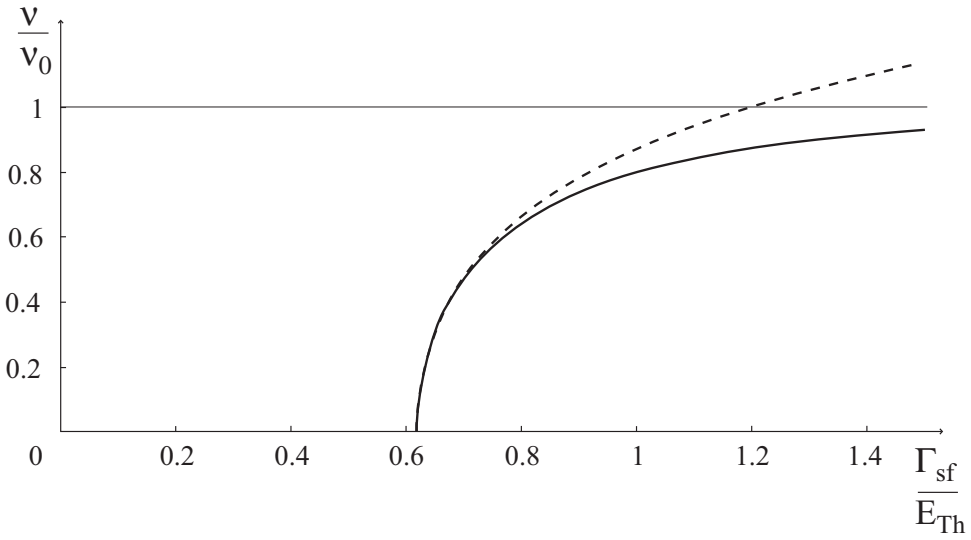

Figure 12: Singularity in the LDoS at x=1: approximation close to Γ_{sf}^{c}.

From the property (A.4), we see directly that $\theta^1 = \frac{\pi}{2}$ always satisfies this equation. Using property (A.6), we can write the boundary condition for θ^1

$$1 - \cos^2\theta^1 = 1 - \cos^2\theta^1 \mathrm{sn}^2[-2\sqrt{\Gamma_{sf}}, \cos\theta^1]. \tag{8.11}$$

This equation can be satisfied if

$$\mathrm{sn}[-2\sqrt{\Gamma_{sf}}, \cos\theta^1] = \pm 1. \tag{8.12}$$

Using the inversion of the elliptic function sn in terms of the incomplete elliptic integral of the first kind F, we obtain

$$\mathrm{sn}[u, k] = \sin\beta \tag{8.13}$$

$$\begin{aligned} \Leftrightarrow u &= F(\beta, k) && (8.14)\\ &= \int_0^\beta \frac{dx}{\sqrt{1 - k^2\sin^2 x}}, && (8.15) \end{aligned}$$

we find

$$2\sqrt{\Gamma_{sf}} = \int_0^{\frac{\pi}{2}} \frac{dx}{\sqrt{1 - \cos^2\theta^1 \sin^2 x}}. \tag{8.16}$$

The critical spin-flip rate where the gap closes which we discussed in the previous section is for $\cos(\theta^1) = 0$. At this point, the constant solution

$\theta = \frac{\pi}{2}$ and the solution of (8.16) merge. We recover therefore the result of the previous section:

$$2\sqrt{\Gamma_{sf}^c} = \frac{\pi}{2} \quad \Rightarrow \quad \Gamma_{sf}^c = \frac{\pi^2}{16}. \tag{8.17}$$

Now, it is possible to find an expression for both the imaginary solution (gap solution) and the real solution (gapless regime) near the closing point. Expanding the integrand in (8.16) near $\cos\theta^1 = 0$ we get:

$$\cos\theta^1 \approx 2\left(\sqrt{\frac{\Gamma_{sf}}{\Gamma_{sf}^c}} - 1\right)^{\frac{1}{2}}. \tag{8.18}$$

Below Γ_{sf}^c, this expression leads to a purely imaginary $\cos\theta^1$ wich corresponds to the second branch of the gap solution we already discussed in section (7.1). Beyond Γ_{sf}^c, we recover the purely real gapless solution of section (7.2).

It is possible to expand the integrand of (8.16) one order further and to get a more accurate expression for the DoS:

$$\cos\theta^1 \approx \frac{2\sqrt{2}}{3}\left[\left(9\sqrt{\frac{\Gamma_{sf}}{\Gamma_{sf}^c}} - 8\right)^{\frac{1}{2}} - 1\right]^{\frac{1}{2}} \tag{8.19}$$

This expression (dashed line on Figure 12) can be compared with the exact solution (solid line on Figure 12) of equation (8.10).

9 Summary

The aim of this work was to study the density of states in disordered superconductor-normal metal junctions when magnetic impurities are present using the Green functions formulation of the BCS theory. In the first part, we have reviewed the description of superconducting materials in the Usadel limit (dirty superconductors) and how this description can be extended to S-N hybrid structures with appropriate boundary conditions for the Usadel equations. Then, we have briefly discussed the solution of the Usadel equations for a semi-infinite S-N system without spin-flip and the apparition of a gap in the DoS of the N-part ("minigap"). If we consider energies much smaller than the gap in the S-part or if the N-part is much more disordered than the S-part, the boundary condition at the S-N interface becomes rigid: we take the bulk superconductor value of the Green function at the S-N interface. After this, we have seen how the effect of magnetic impurities and inelastic scattering can be included as extra terms in the Usadel equations.

The easiest way to get information on the effect of spin-flip and inelastic scattering is to study the linearised Usadel equations. We have considered two different ways of linearising the Usadel equations: close to the zero-energy bulk solution and close to the normal state solution. We have discussed how a small spin-flip scattering rate can be reduced to an effective inelastic scattering rate and contribute to a finite subgap density of states. The Usadel equations can be integrated once. Working with this first integral, we have seen that it is not possible to find a zero-DoS solution if inelastic scattering is present. Neglecting inelastic scattering, we have studied the influence of spin flip on the minigap. The minigap (maximal energy compatible with a zero-DoS solution) is reduced by scattering on magnetic impurities: we have found the resulting correction for a small spin-flip scattering rate. The method of the first integral allowed us to find a critical value of the spin-flip rate at which the minigap closes and the asymptotic form of the minigap near this point. Finally, we compared our asymptotics for the minigap with the complete numerical curve.
At zero-energy, we have found a complete solution for the Usadel equations in terms of Jacobi elliptic functions. For large spin-flip rates, this solution leads to a DoS saturating to the normal state DoS. Close to the critical spin-flip rate where the minigap closes, we derived the asymptotic form of the local density of states at the interface with vacuum.

In this work, we have shown that the effect of scattering on magnetic impurities on a proximity structure is very similar to its effect on a homogeneous superconductor. The features we have listed above are also present in the homogeneous superconductor, where the superconducting gap Δ is the relevant energy scale instead of the Thouless energy.

References

[1] Kopnin: *Theory of Nonequilibrium Superconductivity*, Oxford University Press, (2001)

[2] Bardeen J., Cooper L.N. and Schrieffer J.R.,Phys. Rev 108, 1175, (1957)

[3] Gor'kov L. P., Sov. Phys. JETP, 36, 1918, (1959).

[4] Abrikosov A. A. and Gor'kov L. P.: *Contribution to the theory of superconducting alloys with paramagnetic impurities.*, Sov. Phys. JETP, 12, 1243, (1961)

[5] Courtois, Charlat, Gandit Mailly & Pannetier: *The spectral conductance of a proximity superconductor and the reentrance effect*, cond-mat/9902014, (1999)

[6] Alexander Altland, B. D. Simons and D. Taras-Semchuk: *Field theory of mesoscopic fluctuations in superconductor/normal-metal systems* , cond-mat/9807371, (1998)

[7] W. Belzig, C. Bruder, and Gerd Schön: *Local density of states in a dirty normal metal connected to a superconductor* , cond-mat/9605039, (1996)

[8] Dmitri A. Ivanov, Raphael von Roten, and Gianni Blatter: *Minigap in a long disordered SNS junction: analytical results*, cond-mat/0204088, (2002)

[9] F. Zhou, P. Charlat, B. Spivak, B.Pannetier: *Density of states in superconductor-normal-superconductor metal junctions*, cond-mat/9707056, (1998)

[10] M. Y. Kupriyanov and V. F. Lukichev: *Influence of boundary transparency on the critical current of "dirty" SS'S structures*, Sov. Phys. JETP 67, 1163, (1988)

[11] Vinay Ambegaokar and Allan Griffin: *Theory of the thermal conductivity of superconducting alloys with paramagnetic impurities*, Phys. Rev. 137, 4A, 1151, (1965)

[12] Venkat Chandrasekhar: *An introduction to the quasiclassical theory of superconductivity for diffusive proximity-coupled systems*, June 2004

[13] P. M. Ostrovsky, M. A. Skvortsov, and M. V. Feigel'man: *Density of states below the Thouless gap in a mesoscopic SNS junction*, cond-mat/0012478, (2001)

[14] E. Bascones: Ph. D. Thesis

[15] Y. Fominov : Ph. D. Thesis, cond-mat/0311359, (2003)

[16] Charlat : *Transport et cohérence quantique dans les nanocircuits hybrides supraconducteur-métal*, Ph. D. Thesis, (1997)

[17] D. F. Lawden: *Elliptic Functions and Applications*, Springer, (1989)

[18] P. L. Walker: *Elliptic Functions: a constructive approach*, John Wiley & Sons, (1996)

[19] R. D. Parks: *Superconductivity*, Marcel Dekker, INC. New-York, (1969)

[20] Tinkham: *Introduction to Supercondutivity*, Mc Graw Hill, (1996)

[21] P. G. De Gennes: *Superconductivity of Metals and Alloys*, W.A Benjamin. INC. New-York, (1966)

[22] A.A. Abrikosov, L.P. Gor'kov and I. Y. Dzyaloshinskii: *Quantum Field Theoretical Methods in Statistical Physics*, Pergamon Press, (1965)

[23] A.A. Abrikosov: *Fundamentals of the Theory of Metals*, North-Holland, (1988)

A Exact zero-energy solution for finite Γ_{sf}

First, we briefly discuss the properties of the Jacobi elliptic functions that we will use in this derivation (we follow [17]). There are several approaches to introduce these functions (theta functions or inversion of an elliptic integral, following equation (8.13)). One can show that the three elliptic functions are uniquely determined by the equations:

$$\frac{d}{du}\mathrm{sn}(u,k) = \mathrm{cn}(u,k)\mathrm{dn}(u,k) \tag{A.1}$$

$$\frac{d}{du}\mathrm{cn}(u,k) = -\mathrm{sn}(u,k)\mathrm{dn}(u,k) \tag{A.2}$$

$$\frac{d}{du}\mathrm{dn}(u,k) = -k^2\mathrm{sn}(u,k)\mathrm{cn}(u,k) \tag{A.3}$$

and the initial conditions:

$$\mathrm{sn}(0,k) = 0,\ \mathrm{cn}(0,k) = \mathrm{dn}(0,k) = 1. \tag{A.4}$$

The *argument* u and the *modulus* k can take arbitrary complex values. The functions sn and cn are related to dn by the relations:

$$k\,\mathrm{sn}(u,k) = \sqrt{1-\mathrm{dn}^2(u,k)} \tag{A.5}$$

$$k\,\mathrm{cn}(u,k) = \sqrt{\mathrm{dn}^2(u,k)-k'^2}. \tag{A.6}$$

Here, we introduced the *complementary modulus* k':

$$k^2 + k'^2 = 1. \tag{A.7}$$

After this brief introduction to the Jacobi elliptic functions, we are ready to begin with the derivation of the solution. In this appendix, we show that:

$$\theta(x) = \begin{cases} \arcsin\left[\sin\theta^{\,1}\mathrm{dn}^{-1}\left(2\sqrt{\frac{\Gamma_{sf}}{D_n}}(x-1),\cos\theta^{\,1}\right)\right] & x>0 \\ \theta^{\,s} + 4\arctan\left[\tan\left(\frac{\theta^{\,0}-\theta^{\,s}}{4}\right)\exp\left(\sqrt{\frac{2\Delta}{D_s}}\,x\right)\right] & x<0 \end{cases} \tag{A.8}$$

is a solution of the zero-energy Usadel equations (we neglegt self-consistency and inelastic scattering):

$$\frac{D_{n,s}\partial_x^2\theta}{2} - 2\Gamma_{sf}\Theta(x)\cos\theta\sin\theta + \Delta\Theta(-x)\cos\theta = 0, \tag{A.9}$$

where $\Theta(x)$ is the step function and $\mathrm{dn}^{-1}(u,k)$ denotes $\frac{1}{\mathrm{dn}(u,k)}$. We used the notations $\theta(x=0,1) = \theta^{0,1}$ for the values of the proximity angle at the S-N boundary, respectively at the interface with vacuum. $\theta^{\,s}$ is the value of the

proximity angle in the bulk superconductor. Since we work at zero-energy, we have $\theta^s = \frac{\pi}{2}$.

For $x > 0$ (N-part), we denote $u = 2\sqrt{\frac{\Gamma_{sf}}{D_n}}(x-1)$, $k = \cos\theta^1$ and $k' = \sin\theta^1$. Using these notations and the properties listed in the beginning of this appendix, we can compute the derivatives of (A.8):

$$\partial_x\theta = 2\sqrt{\frac{\Gamma_{sf}}{D_n}}k' \left[\mathrm{dn}^{-2}(u,k) - 1\right]^{\frac{1}{2}} \tag{A.10}$$

For $x = 1$, we can see from the property (A.4) that the boundary condition $\partial_x\theta|_{x=1} = 0$ is satisfied. For the second derivative, we get:

$$\partial_x^2\theta = 4\frac{\Gamma_{sf}}{D_n}k'\mathrm{dn}^{-1}(u,k)\left[1 - k'^2\mathrm{dn}^{-2}(u,k)\right]^{\frac{1}{2}} \tag{A.11}$$

Finally, from equation (A.8) we see that:

$$\mathrm{dn}^{-1}(u,k) = \frac{\sin\theta}{\sin\theta^1} \tag{A.12}$$

Therefore we get:

$$\partial_x^2\theta = 4\frac{\Gamma_{sf}}{D_n}\cos\theta\sin\theta \tag{A.13}$$

which satisfies the Usadel equation (A.9) in the N-part.

The S-part of the solution has been discussed in [7]. We must now use the boundary conditions at the S-N interface to match the S- and the N-part of the solution. The interface transparency (5.2) gives:

$$\theta_-^0 = \theta_+^0 \quad \Rightarrow \quad \sin\theta^0 = \sin\theta^1\mathrm{dn}^{-1}[-2\sqrt{\frac{\Gamma_{sf}}{D_n}}, \cos\theta^1] \tag{A.14}$$

The conservation of the quasiparticle current (5.2) can also be written in terms of the proximity angle:

$$\sigma_s\partial_x\theta_-^0 = \sigma_n\partial_x\theta_+^0 \tag{A.15}$$

After a straightforward calculation, we get for the derivative of the S-part solution at $x = 0$:

$$\partial_x\theta_-^0 = 2\sqrt{\frac{2\Delta}{D_s}}\sin\left(\frac{\theta^0 - \theta^s}{2}\right). \tag{A.16}$$

The derivative of the N-part solution has already been calculated in equation (A.10):

$$\partial_x\theta_+^0 = 2\sqrt{\frac{\Gamma_{sf}}{D_n}}\sin\theta^1\left[\mathrm{dn}^{-2}\left(-2\sqrt{\frac{\Gamma_{sf}}{D_n}}, \cos\theta^1\right) - 1\right]^{\frac{1}{2}} \tag{A.17}$$

Using equation (A.12), we get:

$$\partial_x \theta_+^0 = 2\sqrt{\frac{\Gamma_{sf}}{D_n}} \left[\sin^2\theta^0 - \sin^2\theta^1\right]^{\frac{1}{2}} . \tag{A.18}$$

Finally, the boundary condition (A.15) becomes

$$\sin(\frac{\theta^0 - \theta^s}{2}) = \gamma\sqrt{\frac{\Gamma_{sf}}{2\Delta}}\sqrt{\sin^2\theta^0 - \sin^2\theta^1} \tag{A.19}$$

where $\gamma = \frac{\sigma_n/\sigma_s}{\sqrt{D_n/D_s}}$.

B Exact solution for $\Gamma_{sf} = 0$

In this appendix, we briefly introduce the finite energy solution derived in [6]. This solution can be directly extended to include inelastic scattering. Without spin-flip, the Usadel equation (3.59) for the S-N junction (we neglegt self-consistency) can be written

$$\frac{D_{n,s}\partial_x^2\theta}{2} + (i\epsilon - \Gamma_{in})\sin\theta + \Delta\Theta(-x)\cos\theta = 0. \tag{B.1}$$

The solution of this equation for a finite size N-part can be expressed in terms of Jacobi elliptic functions. For an introduction to these functions, the reader may refer to [17] and to the discussion of appendix A. Equation (B.1) is solved for

$$\theta(x) = \begin{cases} 2\arcsin\left[\sin\frac{\theta^1}{2}\mathrm{sn}\left(-\sqrt{\frac{2(i\epsilon-\Gamma_{in})}{D_n}}(x-1) + K(\sin\frac{\theta^1}{2}), \sin\frac{\theta^1}{2}\right)\right] & x > 0 \\ \theta^s + 4\arctan\left[\tan\left(\frac{\theta^0-\theta^s}{4}\right)\exp\left(\sqrt{\frac{2\sqrt{\Delta^2-(i\epsilon-\Gamma_{in})^2}}{D_s}}\, x\right)\right] & x < 0 \end{cases} \tag{B.2}$$

where K represents the complete elliptic integral of the first kind:

$$K(k) = F(\frac{\pi}{2}, k) = \int_0^{\frac{\pi}{2}} \frac{d\varphi}{\sqrt{1-k^2\sin^2\varphi}}. \tag{B.3}$$

The parameters $\theta^0 = \theta(x=0)$ and $\theta^1 = \theta(x=1)$ can be obtained from the boundary conditions

$$\theta_-^0 = \theta_+^0 \tag{B.4}$$

$$\Rightarrow \sin\frac{\theta^0}{2} = \left[\sin\frac{\theta^1}{2}\mathrm{sn}\left(\sqrt{\frac{2(i\epsilon-\Gamma_{in})}{D_n}} + K(\sin\frac{\theta^1}{2}), \sin\frac{\theta^1}{2}\right)\right] \tag{B.5}$$

The conservation of the quasiparticle current (5.2) can also be written in terms of the proximity angle:

$$\sigma_s\partial_x\theta_-^0 = \sigma_n\partial_x\theta_+^0 \tag{B.6}$$

$$\Rightarrow \sin(\frac{\theta^0-\theta^s}{2}) = \gamma\sqrt{\frac{\Gamma_{in}-i\epsilon}{\sqrt{\Delta^2+(i\epsilon-\Gamma_{in})^2}}}\sqrt{\sin^2\frac{\theta^0}{2} - \sin^2\frac{\theta^1}{2}} \tag{B.7}$$

recall that $\gamma = \frac{\sigma_n/\sigma_s}{\sqrt{D_n/D_s}}$. From this equation, we see that the boundary conditions become "rigid" ($\theta^0 = \theta^s$) if the N-part is much more disordered that the S-part or if the superconducting gap Δ is much larger than the energies we consider. These conditions are fulfilled if

$$D_n \ll D_s \tag{B.8}$$

$$\text{or} \quad \Delta \gg E_{Th}. \tag{B.9}$$

C Gap curve close to Γ_{sf}^{c}

In this appendix, we derive the asymptotic form of the gap curve given in section (7.3.2). Using the method of the first integral, we showed previously that the minigap E_g was the maximal energy compatible with equation (7.7):

$$2\sqrt{\Gamma_{sf}} = \int_0^{\Theta^1} \frac{1}{\left[\left(\sinh^2\Theta^1 - \sinh^2\Theta\right) + \frac{\epsilon}{\Gamma_{sf}}\left(\sinh\Theta^1 - \sinh\Theta\right)\right]^{1/2}} d\Theta. \tag{C.1}$$

Setting

$$x = \sinh\Theta \tag{C.2}$$
$$x_1 = \sinh\Theta^1 \tag{C.3}$$
$$\text{and} \quad 2\alpha = \epsilon/\Gamma_{sf}, \tag{C.4}$$

we get

$$2\sqrt{\Gamma_{sf}} = \int_0^{x_1} \frac{1}{\sqrt{\left(x_1^2 - x^2\right) + 2\alpha\left(x_1 - x\right)}} \cdot \frac{1}{\sqrt{1+x^2}} dx. \tag{C.5}$$

Now we introduce another variable $\bar{x} = x + \alpha$. Equation $(C.5)$ becomes :

$$2\sqrt{\Gamma_{sf}} = \int_\alpha^{\bar{x}_1} \frac{1}{\sqrt{\bar{x}_1^2 - \bar{x}^2}} \cdot \frac{1}{\sqrt{1+(\bar{x}-\alpha)^2}} d\bar{x}. \tag{C.6}$$

The integral in the r.h.s. of the equation is a function of $\bar{x}_1$ and α. We denote this function $Y(\bar{x}_1, \alpha)$. To find the minigap, we have to find the maximal value of this function (we get the maximal Γ_{sf} for a given energy). At the critical Γ_{sf}, we have

$$\epsilon = 0 \quad \Rightarrow \quad \alpha = 0 \quad \text{and} \quad x = \bar{x}. \tag{C.7}$$

And the critical spin-flip rate is given by the maximum taken over $\bar{x}_1$ of the expression

$$Y(\bar{x}_1, \alpha)|_{\alpha=0} = \int_0^{\bar{x}_1} \frac{1}{\sqrt{\bar{x}_1^2 - \bar{x}^2}} \cdot \frac{1}{\sqrt{1+\bar{x}^2}} d\bar{x} \tag{C.8}$$
$$= \int_0^1 \frac{1}{\sqrt{1-z^2}} \cdot \frac{1}{\sqrt{1+(\bar{x}_1 z)^2}} dz. \tag{C.9}$$

It is clear that the integral of equation (C.9) is maximal for $\bar{x}_1 = 0$, therefore we recover the result

$$E_g(\Gamma_{sf}^c = \frac{\pi^2}{16}) = 0. \tag{C.10}$$

The next step is to go to finite energies and expand Y in the small α. We write

$$Y(\bar{x}_1,\alpha) = Y(\bar{x}_1,\alpha)|_{\alpha=0} + \frac{\partial Y(\bar{x}_1,\alpha)}{\partial\alpha}|_{\alpha=0}\,\alpha, \tag{C.11}$$

where

$$\frac{\partial Y(\bar{x}_1,\alpha)}{\partial\alpha}|_{\alpha=0} = -\frac{1}{\bar{x}_1} - \int_0^{\bar{x}_1} \frac{d\bar{x}}{\sqrt{\bar{x}_1^2-\bar{x}^2}}\frac{\bar{x}}{(1+\bar{x}^2)^{3/2}}. \tag{C.12}$$

For a small α, the maximum of Y is expected to be close to the zero-energy value $\bar{x}_1 = 0$. The second term in equation (C.12) can therefore be neglected:

$$\int_0^{\bar{x}_1} \frac{d\bar{x}}{\sqrt{\bar{x}_1^2-\bar{x}^2}}\frac{\bar{x}}{(1+\bar{x}^2)^{3/2}} \approx \int_0^{\bar{x}_1} \frac{\bar{x}}{\sqrt{\bar{x}_1^2-\bar{x}^2}}d\bar{x} = O(\bar{x}_1). \tag{C.13}$$

Now we have to take the maximum of Y over $\bar{x}_1$ using equation (C.12). This results in

$$\frac{\partial}{\partial\bar{x}_1}\left[Y(\bar{x}_1,\alpha)|_{\alpha=0}\right] = -\frac{\alpha}{\bar{x}_1^2}. \tag{C.14}$$

From expression (C.9), we have

$$\frac{\partial}{\partial\bar{x}_1}\left[Y(\bar{x}_1,\alpha)|_{\alpha=0}\right] = -\underbrace{\int_0^1 \frac{z^2}{\sqrt{1-z^2}}dz}_{\pi/4=\sqrt{\Gamma_{sf}^c}}\,\bar{x}_1, \tag{C.15}$$

and therefore the maximum satisfies

$$\hat{\bar{x}}_1 = \left[\frac{\alpha}{\sqrt{\Gamma_{sf}^c}}\right]^{1/3}. \tag{C.16}$$

Finally, substituting this result in equation (C.11) we get

$$Y(\hat{\bar{x}}_1,\alpha) - Y(\hat{\bar{x}}_1,\alpha)|_{\alpha=0} = -\left(\Gamma_{sf}^{c\,1/4}\alpha\right)^{2/3} \tag{C.17}$$

Close to $x_1 = 0$ (for small α), we see from (C.9) that $Y(\bar{x}_1,\alpha)|_{\alpha=0}$ is given by :

$$Y(\bar{x}_1,\alpha)|_{\alpha=0} \approx \int_0^1 \frac{1}{\sqrt{1-z^2}}\left(1-\frac{(\bar{x}_1 z)^2}{2}\right)dz \tag{C.18}$$

Using (C.16) one more time and the definition of α (C.4) we get

$$E_g = \frac{2^{7/2}}{3^{3/2}\sqrt{\Gamma_{sf}^c}}\left[\sqrt{\Gamma_{sf}^c}-\sqrt{\Gamma_{sf}}\right]^{3/2}\Gamma_{sf}. \tag{C.19}$$

Writing $\Gamma_{sf} = \Gamma_{sf}^c - \delta\Gamma_{sf}$, we expand in the small $\delta\Gamma_{sf}$ to find the asymptotic form of equation (C.19):

$$E_g = 2\left(\frac{2}{3}\right)^{3/2}\left[\delta\Gamma_{sf}\right]^{3/2}, \tag{C.20}$$

which is the result given in section (7.3.2).